COORDINATION CHEMISTRY REVIEWS

ELSEVIER

Structural aspects of metal–amide complexes

O. Clement, B.M. Rapko, B.P. Hay *

*Environmental Molecular Science Laboratory, Pacific Northwest National Laboratory,
P.O. Box 999, Richland, WA 99352, USA*

Contents

Abstract

An exhaustive survey of crystal structure data on simple amides and metal complexes containing monodentate amide ligands has been performed. Statistical analysis of structural features are reported as a function of the degree of alkylation of the amide functional group, the type of metal ion in the amide complex, and the type of binding to the metal ion. Average values are reported for bond lengths, bond angles, and torsional angles. Orientational preferences of the coordinated amide ligand are discussed in terms of M–O–C bond angles and M–O–C–N torsion angles. © 1998 Elsevier Science S.A.

Keywords: Amide; Metal complex; Coordination compound; Structure

* Corresponding author. Tel: +1 509 3726239; Fax: +1 509 3756631; e-mail: ben.hay@pnl.gov

1. Introduction

Amides are a class of molecules important to several chemical disciplines. Not only do they comprise a major functional group in organic chemistry [1] but they form key linkages in natural macromolecules such as proteins and polypeptides [2] and synthetic macromolecules such as nylons and Kevlar®. Molecules containing the amide functionality are potentially useful in a variety of applications, including their use as complexing agents for the selective extraction of f-elements [3–32] and of precious metals [17,22,23,15], and as improved ligands for magnetic resonance imaging (MRI) agents [33–36].

In a previous review of metal amide coordination chemistry, Sigel and Martin [2] provided a summary of the structure and stability of metal amide complexes with a strong emphasis on metal complexes containing proteins and peptides. Experimental stability constant data, kinetic information, spectroscopic (IR, NMR, ESR, and electronic) measurements, circular dichroism spectroscopy and some data from X-ray crystal structures were used to examine amide metal interactions in these polydentate ligands. The X-ray structural data were primarily reviewed to determine the denticity of polyfunctional ligands and to identify which atoms in the amide were bound to the metal ion. However, some information was provided regarding changes in the amide bond lengths upon metal coordination; specifically an increase in the carbonyl carbon to oxygen (C_a=O) bond of 0.03 Å and a decrease in the carbonyl carbon to nitrogen (C_a–N) bond length of 0.025 Å following binding of peptides to metal ions through the amide nitrogen.

Several aspects of the X-ray structural data were not described in this prior review. Such unreviewed structural features include the metal to oxygen bond distances for oxygen coordinated compounds and directional preferences of the amide metal bonding such as metal–amide bond angles and metal–amide torsional angles. Through a systematic examination of relevant crystallographic data it is often possible to discover geometric preferences and trends over series of compounds [37].

Previous work has demonstrated the importance of metal–ligand bond directional preferences in understanding metal complex structure, as well as the relationship between structure and metal complex stability. Specific geometric preferences of the nitrogen donor in metal–amine complexes [38] and the oxygen donor in metal–ether complexes [39] are key to understanding the role of ligand architecture on metal complex stability. In this review, the results of a systematic search of the Cambridge structural database (CSD) [40] have been analyzed to help define the structural features of metal–amide coordination chemistry. Information from crystal structures of metal-coordinated amides has been compiled and evaluated to detect the geometrical preferences of the amide donor group following coordination to a metal. To the best of our knowledge, this review represents the first such comprehensive examination of metal amide compounds.

Several restrictions were imposed on the selection of data used in this analysis to help isolate and focus on the structural aspects of the amide–metal interaction. The evaluation of the results from this CSD search was limited to monodentate amide ligands with aliphatic carbon atoms attached α and β to the amide carbonyl and

N,N-dimethylformamide   acetamide   N-alkylacetamide

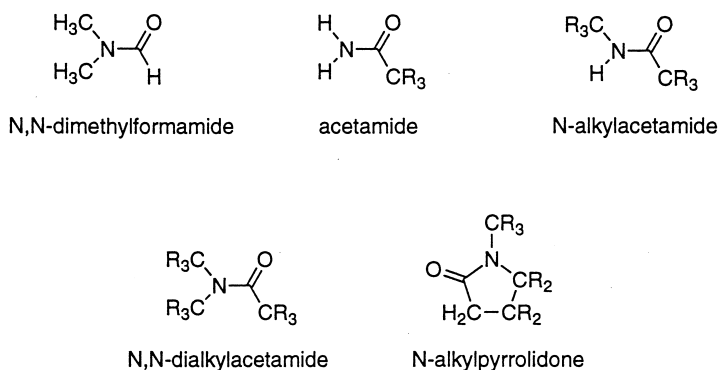N,N-dialkylacetamide   N-alkylpyrrolidone

Fig. 1. Amide structural types covered in this review.

nitrogen atoms. The limitation to monodentate amide ligands was introduced to avoid the presence of chelate rings, which would add the various structural preferences imposed by the chelate ring to those of the amide and thus possibly obscure the nature of the metal amide interaction. The limitation requiring only aliphatic carbons attached to the amide groups was introduced to minimize any structural impact caused by inductive effects and changing amide basicity. In addition, with one exception, amides containing cyclic structure were excluded from consideration. The exception occurs with *N*-alkylpyrrolidones where a sufficient number of examples were present for anlaysis.

In the following discussion, the data are divided into five types of amides which are distinguished by their degree of alkylation as shown in Fig. 1. The structural features of the free amide ligands are presented in Section 2. The structural features of oxygen-bound amide metal complexes are presented in Section 3 where the data for each type of amide are further divided with respect to metal ion type, e.g. group 1, group 2, groups 3 and 4, transition metals (groups 5 through 12) and the lanthanides and actinides. The structural features of nitrogen-bound amide metal complexes are discussed in Section 4.

2. The free amide structure

This section summarises and discusses the structural aspects of the free amide ligand. This allows for a subsequent comparison of the structural features of uncoordinated amides with metal-coordinated amides. Such comparisons, presented in subsequent sections, reveal the extent to which coordination to metal ions alters amide structure. The structural features of the five amide types defined in Fig. 1 were averaged and the results are summarized in Table 1.

The average bond lengths are tightly clustered with standard deviations ranging from 0.01 to 0.03 Å. At this level of precision, there is no significant variation in bond length with change in alkyl substitution. The lengths of the $C_a{=}O$

Table 1
Amide structural features in the absence of metal ions[a]

Feature	N,N-dimethyl-formamide	Acetamide	N-alkyl-acetamide	N,N-dialkyl-acetamide	N-alkyl-pyrrolidone
Number of structures	78	128	90	28	12
$C_a{=}O$	1.23(2)	1.24(1)	1.23(1)	1.23(1)	1.23(2)
$C_a{=}O$	1.32(2)	1.33(2)	1.34(2)	1.34(2)	1.33(2)
C_a–C	—	1.51(2)	1.50(1)	1.52(2)	1.50(2)
N–CR_3	1.44(2)	—	1.46(1)	1.46(2)	1.45(1)
C–C_a–O	—	121(1)	122(1)	120(1)	126(1)
N–C_a–O	125(2)	122(1)	122(1)	122(1)	125(1)
Na–C_a–C	—	117(1)	116(1)	119(2)	109(1)
C–N–C_{cis}	120(2)	—	123(2)	119(1)	123(2)
C–N–C_{trans}	122(2)	—	—	124(2)	115(2)
C_{cis}–N–C_{trans}	118(2)	—	—	117(2)	122(2)
Average deviation from plane[b]	0.01(1)	0.005(7)	0.02(1)	0.02(1)	0.02(1)

[a]Distances are given in Å and bond angles are given in degrees. Standard deviations (1σ) are given in parentheses. Labels are as follows: C_a, sp^2 carbonyl carbon; C_{cis}, carbon *cis* to oxygen; C_{trans}, carbon *trans* to oxygen.
[b]Average deviation from the best plane through O, C_a, N and any carbon atoms directly attached to these atoms.

(1.23–1.24 Å) and C_a–N (1.32–1.34 Å) bonds are of interest. For comparison, typical $C_a{=}O$ lengths for analogous ketones are 1.21–1.23 Å [41], and typical C–N lengths for simple aliphatic amines are 1.45–1.47 Å [42]. This phenomenon can be rationalized by invoking a substantial contribution of the charge-separated resonance form shown in Fig. 2 [43,44].

In the gas phase, the amide $C_a{=}O$ lengths are shorter (1.22 Å) and the C_a–N lengths are longer (1.38 Å) [1,45,46] than in condensed phases, a phenomenon also consistent with a substantial contribution of the charge-separated resonance form for the amide. As the dielectric constant of the medium increases, the resonance form with charge separation becomes more important and the $C_a{=}O$ bond gains more single bond character while the C_a–N bond gains more double bond character. Consistent with the presence of substantial double bond character to the C_a–N bond, the barrier to C_a–N rotation is between 15 and 20 kcal/mol [43,45,47].

The partial double bond character of the C_a–N bond is also responsible for the rigid, nearly planar, structure of the amide moiety. As seen in Table 1, the average deviation from the best plane through the N, $C_a{=}O$, and any attached carbon atoms is 0.02 Å or less. In addition, for the tertiary amide, summation of the bond angles around nitrogen gives a value of 360°, consistent with a planar amide structure.
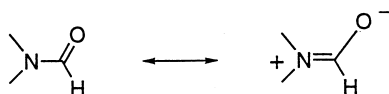

Fig. 2. Standard (left) and charge separated (right) resonance forms for the amide functionality.

Fig. 3. Geometric isomerism in *N*-alkylacetamides.

For *N*-alkylacetamide type structures, the high rotation barrier creates the possibility of two geometric isomers where the *N*-alkyl group is either *cis* or *trans* to the oxygen as shown in Fig. 3. In all 107 structures examined, the alkyl group occurs *cis* to oxygen. This observation is consistent with prior NMR solution studies [48] and theoretical calculations [45]. For *N*–methylacetamide, the *cis* form has been calculated (MM3) to be 2.94 kcal/mol more stable than the *trans* form [45].

3. Oxygen-bound metal–amide complexes

The CSD search revealed a total of 223 monodentate amide ligands bound to metal ions through the oxygen atom. These results are presented by ligand type in accord with Fig. 1, with each ligand type presented separately. In addition, a sample crystal structure that shows typical behavior for that class of metal ions is provided. For each structural type, salient structural features for each metal ion type are averaged and presented in an accompanying table. Structural features of the amide ligand itself and those that describe the metal–amide interaction are included.

Structural changes to the amide ligand following metalation that were examined include the C_a=O and C_a–N bond lengths as well as the angles subtended at the carbonyl carbon. NMR studies have shown that complexation of an amide by metal ions increases the barrier to rotation around C_a–N bond, consistent with an increase in C_a–N double bond character [49]. Such behavior is consistent with binding at oxygen to yield a greater contribution of the charge-separated resonance form shown in Fig. 2 in the amide's structure. This increased contribution should manifest itself in shorter C_a–N and longer C_a=O lengths as compared to the free amide. In addition to amide bond lengths, the O–C_a–N, O–C_a–C angles were examined for changes in amide structure following metal complexation.

Structural features describing the metal–amide interaction that were analyzed include M–O bond lengths, M–O–C_a angles, and M–O–C_a–N torsion angles. The M–O bond lengths were compared with metal ion ionic radii. The M–O–C_a angles were examined to determine if there is a preferred angle at the coordinated amide oxygen. The M–O–C_a–N torsion angles were examined to determine if there is a preferred orientation of the amide with respect to the metal ion.

Often, as will be shown below, the metal ion lies within the plane of the amide. In each table planarity has been described by the percentage of M–L–C_a–N angles that fall within 0 or $180\pm20°$. In the instances where the metal lies in the plane of the amide, geometric isomers are possible and a *cis* or *trans* location of the metal with respect to the amide nitrogen can be specified. However, even in the instances

when the metal amide interaction is not planar, two hemispheres — one the *N*-side of the amide and one opposite the *N*-side of the amide — can be defined. The metal then can be described as being on the same side of the carbonyl bond as the amide nitrogen or on its opposite side. In the former case, the metal possesses a M–O–C_a–N torsion angle of $0 \pm 90°$; in the latter case it possesses a M–O–C_a–N torsion angle of $180 \pm 90°$.

3.1. Metal–dimethylformamide compounds

Because of its widespread use as a solvent, *N,N*-dimethylformamide (DMF) occurs as a ligand and in many metal complexes. Structural features were analyzed for 156 DMF ligands bound to metal ions through the amide oxygen. The results of this analysis are presented in Table 1 as a function of metal ion type. Representative structures for each metal ion type are also presented below.

Several general observations can be taken from Table 2. The anticipated change in C_a=O bond lengths is apparent only for cations of higher charge. With +3 and +4 metal ions there appears, on average, to be some lengthening in C_a=0 bond length (0.01–0.03 Å). However, with the possible exception of the +4 transition metals, no concomitant shortening of the C_a=N length is observed.

On average, metalation results in a slight decrease of 1–2° in the O–C_a–N angle. The behavior of the M–O–C_a angle appears markedly different depending on the type of metal. Not only do the DMF complexes of the divalent transition metals possess smaller M–O–C_a angles than the other types of metal amide complexes but the range of observed angles for the divalent transition metals is much less than with the other metal types. Figs. 4 and 5 illustrate this contrast.

Table 2
Structural features of dimethylformamide when attached to a metal ion through oxygen[a]

Metal type	No. of ligands	C_a=O	C_a–N	O–C_a–N	M–O–C_a	Planar	N-side
None[b]	78	1.23 (2)	1.32 (2)	125(2)	—	—	—
1A	7	1.22 (1)	1.32 (1)	126(1)	145(17)	4/7	2/7
2A	8	1.23 (1)	1.32 (3)	124(2)	130(5)	7/8	1/8
TM^{2+}	85	1.24 (2)	1.32 (1)	124(2)	124(5)	75/85	0/85
TM^{3+}	17	1.26 (2)	1.31 (2)	123(1)	131(15)	15/17	0/17
TM^{4+}	12	1.26 (2)	1.30 (1)	123(1)	138(13)	10/12	0/12
Ln^{3+}	8	1.24 (1)	1.32 (2)	124(2)	134(13)	4/8	0/8
UO$_2^{2+}$	10	1.24 (2)	1.31 (3)	123(2)	134(7)	8/10	0/10
An^{4+}	15	1.25 (4)	1.32 (3)	123(3)	138(6)	9/15	0/15

[a]Distances are given in Å and bond angles are given in degrees. Standard deviations (1σ) are given in parentheses. The orientation of the amide is classified as planar if the M–O–C_a–N torsion angle is either $0 \pm 20°$ or $180 \pm 20°$. The position of the metal ion is classified as N-side if the M–O–C_a–N torsion angle is $0 \pm 90°$. Metal ions: 1A (Li$^+$, Na$^+$), 2A (Mg^{2+}, Ca^{2+}), TM^{2+} (Mn^{2+}, Fe^{2+}, Co^{2+}, Ni^{2+}, Cu^{2+}, Zn^{2+}, MoO$_2^{2+}$, Cd^{2+}, Pt^{2+}), TM^{3+} (V^{3+}, Cr^{3+}, Mn^{3+}, Fe^{3+}, Ru^{3+}, Rh^{3+}, Re^{3+}, Ln^{3+} (La^{3+}, Nd^{3+}, Tb^{3+}), TM^{4+} (Ti^{4+}, V^{4+}, Zr^{4+}), An^{4+} (U^{4+}, Th^{4+}).
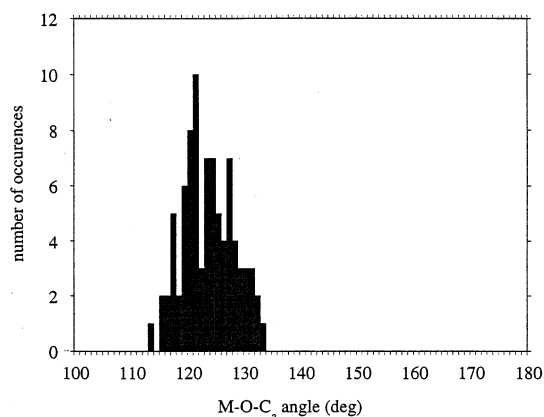[b]Values taken from Table 1.

Fig. 4. Frequency plot of M–O–C_a angles found for DMF-divalent transition metal compounds.
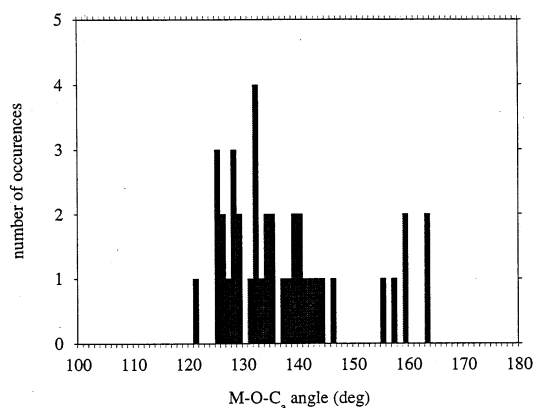

Fig. 5. Frequency plot M–O–C_a angles found for DMF–metal compounds (excluding divalent transition metals).

A similar metal type dependence is observed with respect to the planarity of the metal with the amide ligand. As shown in Figs. 6 and 7, the divalent transition metals show a strong preference for a planar orientation of the metal and amide. Although a preference for planar orientation for the other metals is also found, the preference appears to be weaker as the range of observed torsion angles is much greater.

In the planar cases the metal is always *trans* to N, as shown in Fig. 8. This is readily understood when one considers that the *cis* isomer would contain a highly unfavourable steric interaction between the metal ion and a N–CH_3 group. Consequently, when the metal is in the plane of the amide the metal is always found *trans* to nitrogen. However, in those instances where the metal and amide are nonplanar there are a few examples where the metal does enter the N hemisphere.
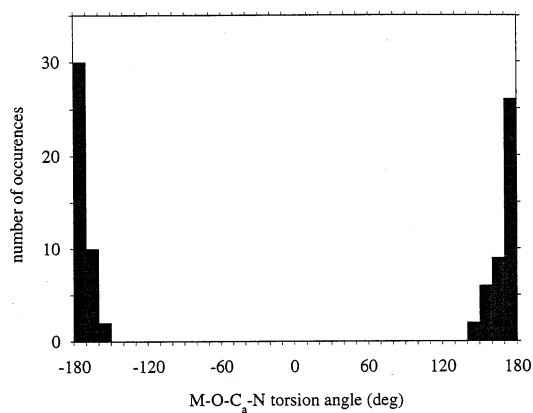
Fig. 6. Frequency plot of M–O–C–N torsion angles for DMF-divalent transition metal compounds.
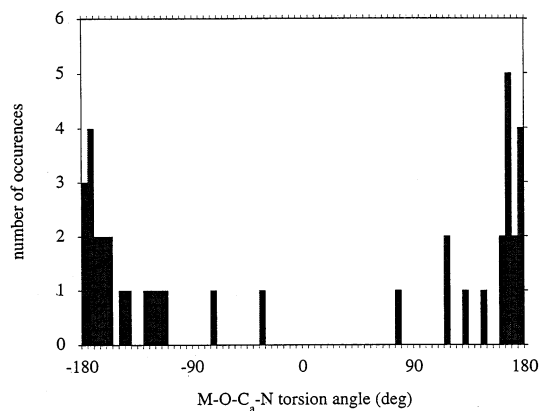
Fig. 7. Frequency plot of M–O–C–N torsion angles for DMF–metal compounds (excluding divalent transition metals).
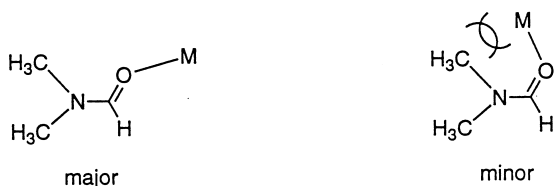

Fig. 8. Metal position in DMF–metal compounds.

This is possible when the unfavourable steric interactions are reduced due to: (1) a long M–O length; and (2) a large M–O–C_a angle.

Bond lengths can often be estimated by summation of a metal ion contribution with a ligand donor contribution. Assuming the amide ligand contributes a constant
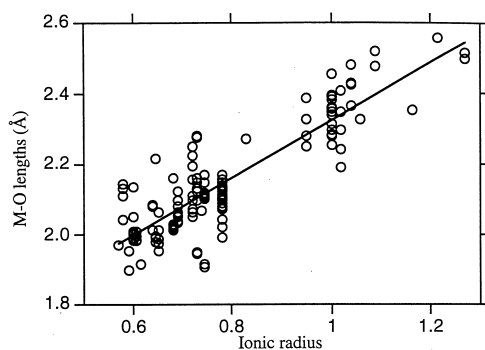
Fig. 9. Plot of M–O versus ionic radius for *O*-bound DMF–metal complexes.

length to the observed metal amide bond lengths a plot of the total metal–amide bond length against metal radii would be expected to possess a slope of 1 and its *y*-intercept (metal radius of 0 Å) would indicate the amide's contribution to the metal–amide bond. Fig. 9 shows a plot of the observed M–O(amide) bond length versus Shannon's ionic radii [50] for metal ions with the coordination numbers found in their structures. Although the expected behavior is not observed, Fig. 9 reveals a clear correlation between the ionic radii and the observed M–O(amide) bond lengths. A least squares linear regression of the data results in the following equation:

$$y = 1.51 + 0.82x; \quad R = 0.88.\tag{1}$$

3.1.1. Specific examples

(a) Alkali metal ions: there are four known structures of alkali metal complexes containing one or more *O*-bound DMF ligand(s) [51–53]. A representative example is shown in Fig. 10 for the cationic complex, $[Na(15\text{-crown-}5)(DMF)_2]^+$ [52]. In the crystal structure of this complex, the average amide $C_a{=}O$ and $C_a{-}N$ bond lengths are ca. 1.21 and 1.32 Å, respectively. The $O{-}C_a{-}N$ angle for free DMF of

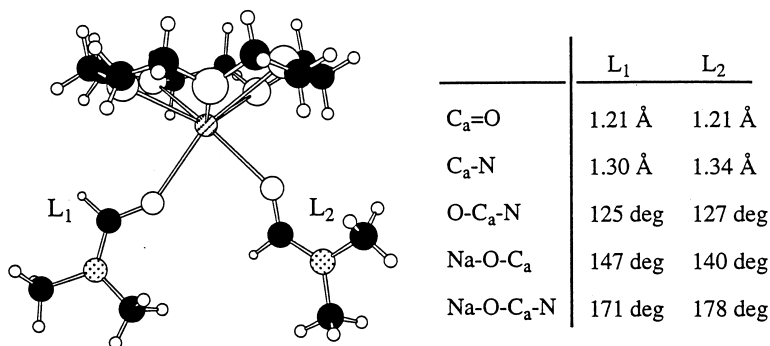|	L_1	L_2
$C_a{=}O$	1.21 Å	1.21 Å
$C_a{-}N$	1.30 Å	1.34 Å
$O{-}C_a{-}N$	125 deg	127 deg
$Na{-}O{-}C_a$	147 deg	140 deg
$Na{-}O{-}C_a{-}N$	171 deg	178 deg

Fig. 10. X-ray crystal structure of the cation $[Na(15\text{-crown-}5)(DMF)_2]^+$.

$125 \pm 1°$ is unaffected by coordination to the Na^+ ion (126°). The Na–O(amide) bond lengths are 2.35 and 2.41 Å, and the corresponding Na–O–C_a angles are 140 and 147°, respectively. The Na–O–C_a–N torsional angle of ca. 175° depicts a planar torsional preference in this complex; however, such planar preferences were only found in about half of the alkali metal ion–DMF structures (Table 2).

(b) Alkaline earth metal ions: the crystal structures of five monodentate oxygen-bound amide complexes of Group 2 metals have been reported [54–58]. These complexes are those formed with Mg^{2+} [55,56] and Ca^{2+} [54,57,58] ions. The coordination polyhedron around these ions is mostly octahedral; a seven coordinate bridged dinuclear Ca^{2+}–DMF complex has also been reported [58]. As a representative example (Fig. 11), the crystal structure of an octahedral Ca^{2+}–DMF complex, $[Ca(DMF)_2(OH_2)_2Cl_2]$, is shown [57]. The average amide $C_a{=}O$ and C_a–N bond lengths in this complex are 1.24 and 1.31 Å, respectively. The observed O–C_a–N angle of 124° differs insignificantly from the average angle in free DMF ($125 \pm 1°$) and so appears unaffected by coordination to the Ca^{2+} ion. The two Ca–O(amide) bond lengths are similar at 2.34 Å, and the corresponding Ca–O–C_a angle is 128°. A planar torsional preference is observed for most alkaline earth–DMF comlexes (Table 2), and this is illustrated by the Ca–O–C_a–N torsional angle of 177° in this complex.

(c) Divalent transition metals: the largest number of reported X-ray crystal structures of metal–DMF complexes are those formed with divalent transition metal ions (Table 2). A representative example is shown for the tetrahedral Zn^{2+} complex, $[Zn(DMF)_2I_2]$ (Fig. 12) [59]. The average amide $C_a{=}O$ and C_a–N bond lengths in this complex are 1.23 and 1.32 Å, respectively. The average O–C_a–N angle for free DMF of $125 \pm 1°$ is only slightly affected by coordination to the Zn^{2+} ion (average O–C_a–N angle of 122°). The short Zn–O(amide) bond length of 1.99 Å is associated with the larger Zn–O–C_a angle of 126°, while the long Zn–O(amide) bond length of 2.01 Å is associated with the smaller Zn–O–C_a angle of 122°. A large proportion

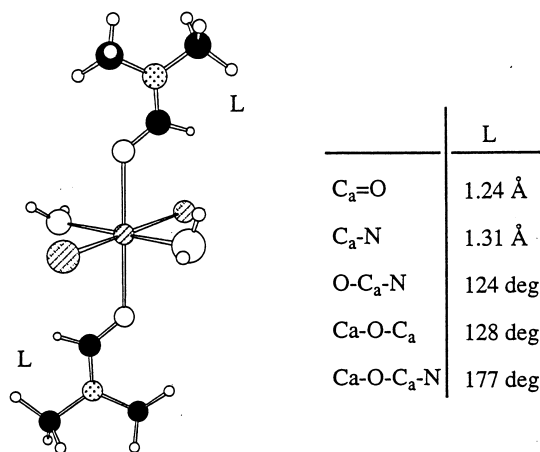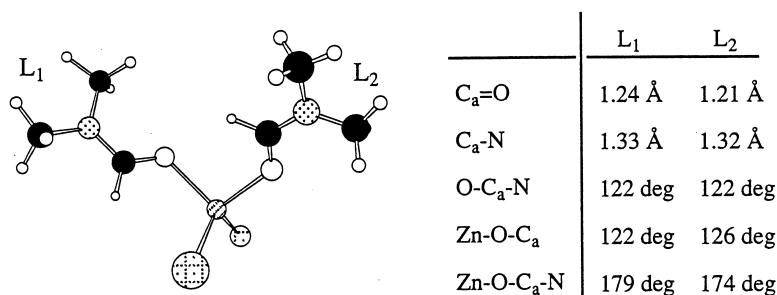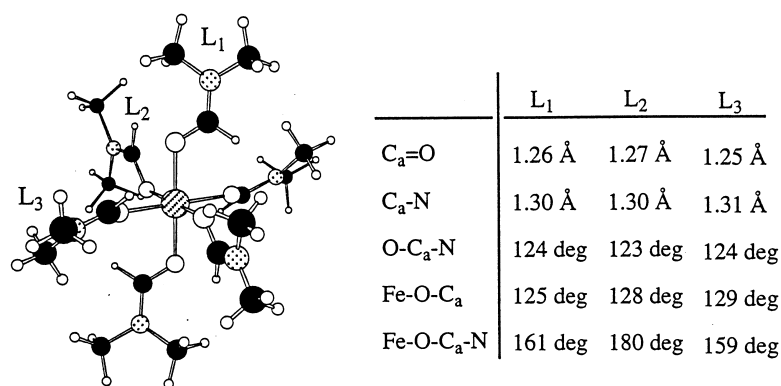|	L
$C_a{=}O$	1.24 Å
C_a-N	1.31 Å
O-C_a-N	124 deg
Ca-O-C_a	128 deg
Ca-O-C_a-N	177 deg

Fig. 11. X-ray crystal structure of $[Ca(DMF)_2(OH_2)_2Cl_2]$.

	L_1	L_2
C_a=O	1.24 Å	1.21 Å
C_a-N	1.33 Å	1.32 Å
O-C_a-N	122 deg	122 deg
Zn-O-C_a	122 deg	126 deg
Zn-O-C_a-N	179 deg	174 deg

Fig. 12. X-ray crystal structure of [Zn(DMF)$_2$I$_2$].

of all the divalent transition metal–DMF complexes whose crystal structures have been determined were found to have a stronger planar torsional preference (Table 2). For example, in the Zn^{2+}–DMF complex shown in Fig. 12, the Zn–O–C_a–N torsional angles range from 174 to 179°.

(d) Trivalent (non-f-block) transition metals: the crystal structures of a number of DMF complexes with trivalent transition metal ions have also been reported [60–67]. The geometrical features in these complexes are similar to those found in the divalent transition metal–DMF complexes described earlier. An example is provided for the octahedral Fe^{3+}–DMF complex, [Fe(DMF)$_6$]$^{3+}$ [66]. In the crystal structure of this complex (Fig. 13), the average amide C_a–O and C_a–N bond lengths are 1.27 and 1.30 Å, respectively. The O–C_a–N angles range between 123° and 124°. Two Fe–O(amide) bond lengths are relatively short (1.98 Å) compared with the other four Fe–O(amide) bond lengths (2.00 Å). Three types of Fe–O–C_a angles present in this complex are centered on 127°. A planar torsional preference is observed for these class of complexes (Table 2); in this instance Fe–O–C_a–N torsional angles range between 160°–180°.

(e) Tetravalent transition metals: higher charged transition metal (+4) complexes of DMF contain Ti^{4+}, V^{4+}, and Zr^{4+} ions [68–70]. A representative example is

	L_1	L_2	L_3
C_a=O	1.26 Å	1.27 Å	1.25 Å
C_a-N	1.30 Å	1.30 Å	1.31 Å
O-C_a-N	124 deg	123 deg	124 deg
Fe-O-C_a	125 deg	128 deg	129 deg
Fe-O-C_a-N	161 deg	180 deg	159 deg

Fig. 13. X-ray crystal structure of the cation [Fe(DMF)$_6$]$^{3+}$.

shown for the octahedral Zr^{4+}–DMF complex, $[Zr(DMF)_2Cl_4]$ (Fig. 14) [70]. In the crystal structure of this complex, the amide C_a=O and C_a–N bond lengths are 1.25 and 1.29 Å, respectively. The O–C_a–N angle is ca. 124°. The Zr–O(amide) bond lengths and Zr–O–C_a angles are 2.05 Å and 150°, respectively. Although a marked planar torsional preference for tetravalent transition metals exists (Table 2), only a borderline preference is observed in this complex, with Zr–O–C_a–N torsional angle of 164°.

(f) Lanthandes: there are seven lanthanide–DMF complexes whose crystal structures have been determined. These are complexes formed with La^{3+} [71–73], Nd^{3+} [74], Eu^{3+} [75,76] and Tb^{3+} [77]. The coordination numbers of the complexes range from 8 to 10. A representative example is provided in Fig. 15 for the complex $[La(18\text{-}crown\text{-}6)(DMF)(isothiocyanate)_3]$ [72]. In the crystal structure of this complex, the amide C_a=O and C_a–N bond lengths are 1.24 and 1.32 Å, respectively.

	L
C_a=O	1.24 Å
C_a-N	1.29 Å
O-C_a-N	123 deg
Zr-O-C_a	150 deg
Zr-O-C_a-N	164 deg
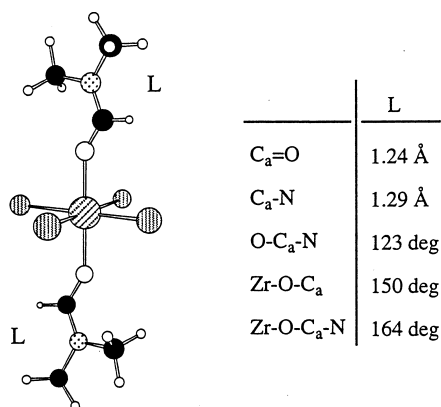
Fig. 14. X-ray crystal structure of $[Zr(DMF)_2Cl_4]$.

	L
C_a=O	1.24 Å
C_a-N	1.32 Å
O-C_a-N	128 deg
La-O-C_a	126 deg
La-O-C_a-N	125 deg

Fig. 15. X-ray crystal structure of $[La(18\text{-}crown\text{-}6)(DMF)(NCS)_3]^{3+}$.

The O–C_a–N angle is ca. 128°. The La–O(amide) bond length is 2.52 Å, while the La–O–C_a angle is 126°. No planar torsional preference is present in this complex (La–O–C_a–N torsional angle is 125°); however, it is observed 50% of the time in Ln–DMF complexes (Table 2).

(g) Actinides — uranyl ion: there are seven UO_2^{2+}–DMF complexes whose X-ray crystal structure determinations have been carried out [78–84]. The coordination numbers in these complexes range from 8 to 10. A representative example is shown in Fig. 16 for the complex, [UO_2(DMF)$_2$(acetato-O,O')(Cl)] [81]. In the crystal structure of this complex, the amide C_a=O and C_a–N bond lengths are 1.24 and 1.29 Å, respectively. The O–C_a–N angle is 124°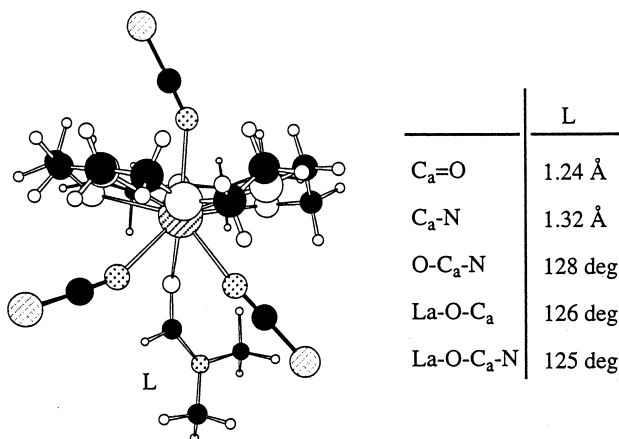. The U–O(amide) bond lengths and U–O–C_a angles are 2.40 Å and 125°, respectively. Although a planar torsional preference is observed in most of UO_2^{2+}–DMF compounds (Table 2), only a border-line preference is present in this complex, with a U–O–C_a–N torsional angle of 160°.

(h) Tetravalent actinides: the five reported crystal structures of actinide–DMF complexes are those of U^{4+} and Th^{4+} [85–89]. These are typically 8- or 9-coordinate complexes. A representative example is shown in Fig. 17 for the complex [U(DMF)$_7$Cl] [89]. In the crystal structure of this complex, the average amide C_a–O and C_a–N bond lengths are 1.27 and 1.32 Å, respectively. The average O–C_a–N angle is 122°. The U–O(amide) bond lengths range from ca. 2.30–2.40 Å, and the U–O–C_a angles range between 132 and 156°. Of the seven DMF ligands bound to the central U^{4+} ion in the complex, three DMF moieties have planar torsional angles (U–O–C_a–N ∼ 160 to 176°), while the other four DMF ligands are nonplanar (U–O–C_a–N ≈ 114–159°).

3.2. Metal–acetamide compounds

There are much less data available on metal–acetamide compounds than are available for metal–DMF compounds. Structural features have been analyzed for

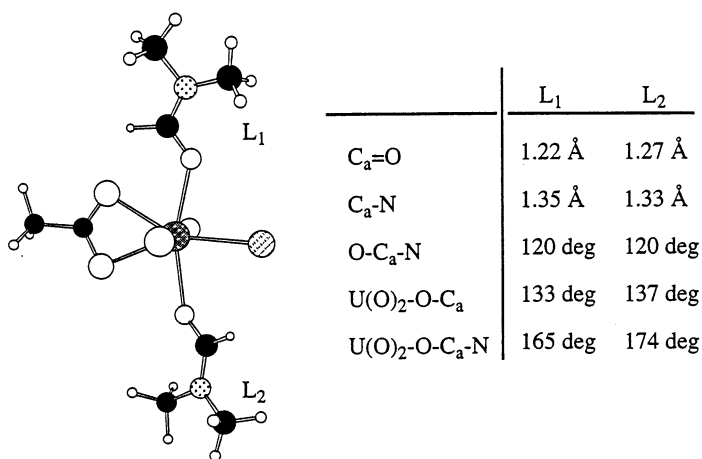|	L₁	L₂
C_a=O	1.22 Å	1.27 Å
C_a-N	1.35 Å	1.33 Å
O-C_a-N	120 deg	120 deg
U(O)$_2$-O-C_a	133 deg	137 deg
U(O)$_2$-O-C_a-N	165 deg	174 deg

Fig. 16. X-ray crystal structure of [UO_2(DMF)$_2$(acetato-O,O')(Cl)].

	L_1	L_2
C_a=O	1.26 Å	1.26 Å
C_a-N	1.32 Å	1.31 Å
O-C_a-N	124 deg	123 deg
U-O-C_a	140 deg	132 deg
U-O-C_a-N	172 deg	148 deg

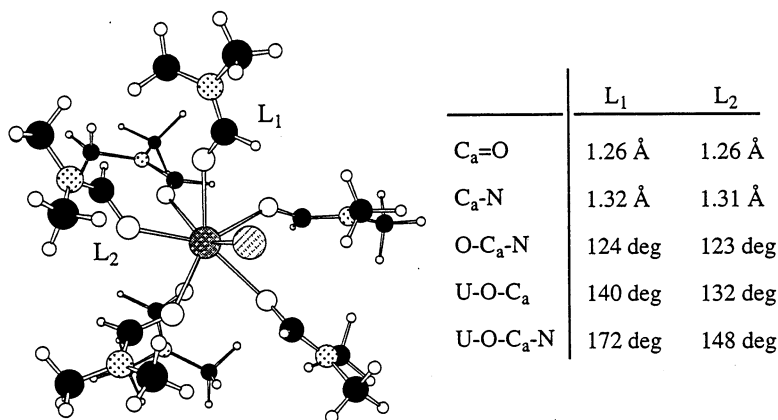Fig. 17. X-ray crystal structure of $[U(DMF)_7Cl]^{3+}$.

the 14 instances where acetamide ligands are bound to metal ions through the amide oxygen. The results of this analysis are presented in Table 3 as a function of two metal ion types observed, divalent transition metal compounds and uranyl compounds. Represntative structures for each metal ion type are also presented below.

Despite the limited amount of structural information that exists for metal acetamide compounds some general observations can be made from Table 3. As was found with the metal–DMF compounds the expected increase in C_a=O bond length is not apparent for divalent transition metal ions. With uranyl ion there appears to be some lengthening in the average C_a–O bond length (0.03 Å). Although shortening of the average C_a–N length is observed, the spread in the bond lengths is such that these differences cannot be considered significant.

On average, metalation results in no change to a slight decrease (0–3°) in the O–C_a–N angle, although the range in values found again makes it difficult to conclude that these observed decreases are significant. No significant changes are observed in the methyl to carbonyl angle. A slight increase (1–2°) is observed in the C–C_a–N angle; again the spread in the data suggests that this may not be significant.

A difference is observed in the average M–O–C_a angles for the two types of metals for which data exists. As with the DMF complexes, the divalent transition metals possess smaller average M–O–C_a angles than do the urnayl compounds and the range of observed angles for the divalent transition metals is much less than with the uranyl compounds.

The planarity of the metal with respect to the amide ligand depends markedly on the metal type. While all examples involving divalent transition metal are planar, none of the uranyl examples are. In contrast to the metal–DMF compounds, if the metal lies in the amide plane then the metal is always *cis* to N. In those instances where the metal and amide are nonplanar there is an equal likelihood that the metal will be found in either hemisphere (Fig. 18).

As with the metal–DMF compounds a plot of the observed M–O(amide) bond

Table 3
Structural feature of acetamide type ligands when attached to a metal ion through oxygen[a]

Metal type	No. of ligands	$C_a{=}O$	$C_a{-}N$	$C_a{-}C$	$O{-}C_a{-}N$	$O{-}C_a{-}C$	$N{-}C_a{-}C$	$M{-}O{-}C_a$	Planar	N-side
None[b]	128	1.24(1)	1.33(2)	1.51(2)	122(1)	121(1)	117(1)	—	—	—
TM^{2+}	10	1.25(1)	1.31(1)	1.49(2)	122(1)	120(1)	118(1)	138(3)	10/10	10/10
UO_2^{2+}	4	1.28(3)	1.30(4)	1.52(8)	120(3)	120(4)	119(2)	145(6)	0/4	2/4

[a]Distances are given in Å and bond angles are given in degrees. Standard deviations (1σ) are given in parentheses. The orientation of the amide is classified as planar if the $M{-}O{-}C_a{-}N$ torsion angle is either $0\pm20°$ or $180\pm20°$. The position of the metal ion is classified as N-side if the $M{-}O{-}C_a{-}N$ torsion angle is $0\pm90°$. Metal ions: TM^{2+} (Co^{2+}, Ni^{2+}, MO_2^{2+}, Re^{2+}).
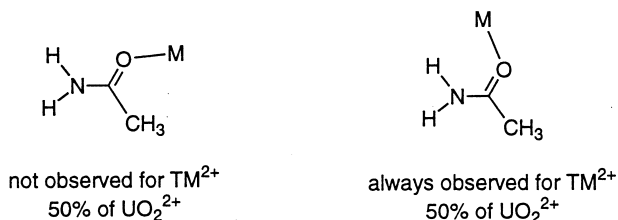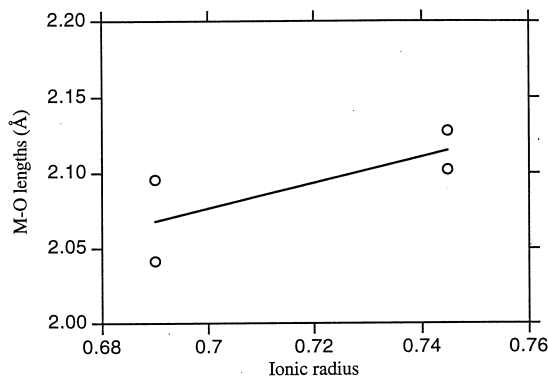[b]Values taken from Table 1.

Fig. 18. Metal position in acetamide compounds.

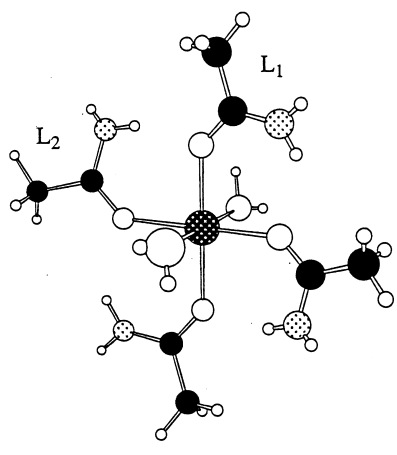Fig. 19. Plot of M–O versus ionic radius for *O*-bound acetamide–metal complexes.

length versus Shannon's ionic radii can be made to examine the amide's contribution to the metal amide bond. Fig. 19 again shows a correlation between the ionic radii and the observed M–O(amide) bond lengths, although the paucity of data cautions against any definitive statements. A least squares linear regression of the data results in the following equation:

$$y = 1.49 + 0.85x; \quad R = 0.73. \tag{2}$$

3.2.1. Specific examples

(a) Transition metals (2+): there are three *O*-bound acetamide complexes with divalent transition metals. These complexes all have octahedral geometries. A representative example is shown in Fig. 20 for the octahedral Co^{2+} complex, $[Co(acetamide)_4(OH_2)_2]^{2+}$ [90]. In the crystal structure of this complex, the C_a–O and C_a–N lengths average 1.25 and 1.30 Å, respectively, while the average C_a–C bond length is ca. 1.50 Å. These bond distances does not differ appreciably from those observed for the free unbound ligand. The apparent lack of structural change in the *O*-bound acetamide ligand upon coordination to transition metals is also reflected in the amide bond angles that lie within the rms deviation of those found in the unbound ligand (Table 3). Two different Co–O(amide) bond lengths are observed. The axial Co–O(Amide) length is 2.13 Å while the equatorial Co–O(amide) bond length is slightly shorter at 2.10 Å. The two Co–O–C_a bond
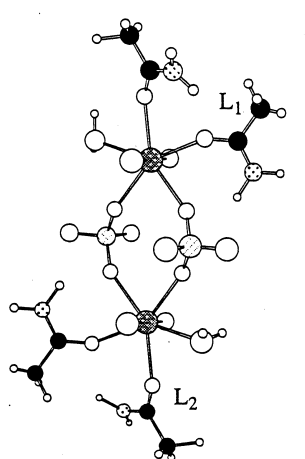
	L_1	L_2
C_a=O	1.24 Å	1.25 Å
C_a-N	1.29 Å	1.31 Å
C_a-C	1.51 Å	1.48 Å
O-C_a-N	123 deg	122 deg
O-C_a-C	119 deg	121 deg
N-C_a-C	119 deg	117 deg
Co-O-C_a	138 deg	138 deg
Co-O-C_a-N	8 deg	3 deg

Fig. 20. X-ray crystal structure of the cation $[Co(acetamide)_4(OH_2)_2]^{2+}$.

angles are similar at ca. 138°. The Co^{2+} ion is oriented *cis* with respect to nitrogen, with torsional angles Co–O–C_a–N ($\sim 8°$). These torsional angles depict the strong planar torsional preference associated with complexes of this class (Table 3).

(b) Actinides — uranyl ion: the only reported oxygen-bound UO_2^{2+}–acetamide complex is the dinuclear complex $[UO_2(acetamide)_2(OH_2)(\mu\text{-sulfato-}O,O')]_2$ (Fig. 20) [91]. In the crystal structure of this complex, the average C_a=O and C_a–N bond lengths in the acetamide ligands L_1 and L_2 (Fig. 21) are 1.25 and 1.30 Å, respectively, while the average C_a–C bond length is ca. 1.50 Å. The bond angles in these ligands are ca. 122, 121 and 118°, for O–C_a–N, O–C_a–C and N–C_a–C, respectively. All four U–O(amide) bond lengths are similar at ca. 2.39 Å. The U–O–C_a angles of 145° and 142° are slightly larger than those found in the corre-

	L_1	L_2
C_a=O	1.25 Å	1.26 Å
C_a-N	1.30 Å	1.30 Å
C_a-C	1.49 Å	1.52 Å
O-C_a-N	121 deg	123 deg
O-C_a-C	121 deg	120 deg
N-C_a-C	118 deg	117 deg
U(O)$_2$-O-C_a	145 deg	142 deg
U(O)$_2$-O-C_a-N	44 deg	23 deg

Fig. 21. X-ray crystal structure of $[UO_2(acetamide)_2(OH_2)(\mu\text{-sulfato-}O,O')_2]_2$.

sponding transition metals. The U–O–C_a–N torsional angles of 44 and 23° indicates the lack of planar torsional preference associated with complexes of this class (Table 3).

3.3. Metal compounds with N-alkylacetamide

As with the metal acetamide compounds, there are much less data available on metal N-alkyl acetamide compounds than are available for metal–DMF compounds. Structural features have been analyzed for the six instances where N-alkyl acetamide ligands are bound to metal ions through the amide oxygen. The results of this analysis are presented in Table 4 as a function of two metal ion types observed, alkali metal (Group 1) compounds and alkaline earth (Group 2) compounds. Representative structures for each metal ion type are also presented below.

The limited amount of structural information available for metal N-alkyl acet-amide compounds cautions against placing too much emphasis on structural changes as a result of metal complexation to N-alkyacetamides. Despite this, some changes in the amide's structure upon metal complexation can be observed in Table 4. The expected increase in C_a=O bond length is not apparent with alkali metal ions, although some lengthening in the average C_a=O bond (0.02 Å) is observed with the alkaline earth compounds. In addition, the C_a–N bond appears to shorten by an average 0.02–0.03 Å.

On average, changes in the O–C_a–N angle vary upon metalation. For alkali metals a decrease of 3° is observed; although for alkaline earth compounds no change is found. Contrary to that found with the acetamide ligands, no significant changes in the methyl to carbonyl angles are observed.

A striking difference exists in the average M–O–C_a for the two types of metal N-alkyl acetamide compounds. The alkali metal N-alkylacetamide complex possesses an almost linear (175°) M–O–C_a angle whereas the M–O–C_a angle for the alkaline earth compounds has a value much closer (145°) to those previously discussed. The presence of a linear M–O–C_a angle in the alkali metal compound demands planarity

Table 4
Structural features of N-alkylacetamide type ligands when attached to a metal ion through oxygen[a]

Metal type	No. of ligands	C_a=O	C_a–N	C_a–C	O–C_a–N	O–C_a–C	N–C_a–C	M–O–C_a	Planar	N-side
None[b]	90	1.23(1)	1.34(2)	1.50(2)	122(1)	122(1)	116(1)	—	—	—
1A[c]	1	1.23	1.32	1.59	119	124	117	175	1/1	—
2A	5	1.25(1)	1.31(2)	1.54(5)	122(2)	121(2)	116(1)	145(7)	3/5	0/5

[a]Distances are given in Å and bond angles are given in degrees. Standard deviations (1σ) are given in parentheses. The orientation of the amide is classified as planar if the M–O–C_a–N torsion angle is either 0±20° or 180±20°. The position of the metal ion is classified as N-side if the M–O–C_a–N torsion angle is 0±90°. Metal ions: 1A (Li$^+$), 2A (Mg^{2+}, Ca^{2+}).
[b]Values taken from Table 1.
[c]Standard deviations cannot be reported for one ligand. When the M–O–C_a angle becomes linear, the M–O–C_a angle becomes planar by definition.
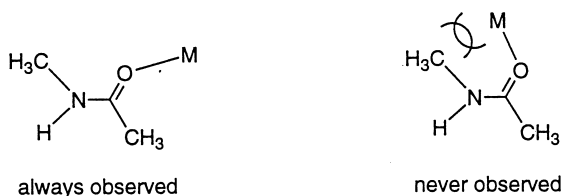
Fig. 22. Metal position in *N*-alkylacetamide compounds.

of the metal with respect to the amide ligand and prevents, by definition, assignment of the metal to either of the hemispheres defined by the carbonyl group. Unlike the divalent transition metal compounds with acetamide (Table 3), the alkaline earth compounds of *N*-alkylacetamides all have the metal *trans* to nitrogen (Table 4), presumably due to the increased steric demands around the amide nitrogen upon alkylation (Fig. 22).

A plot of the observed M–O(amide) bond length versus Shannon's ionic radii for the *N*-alkyl acetamide compounds is shown in Fig. 23. A correlation between the ionic radii and the observed M–O(amide) bond lengths is again observed. A least-squares linear regression of the data results in the following equation:

$$y = 1.59 + 0.62x; \quad R = 0.94. \tag{3}$$

3.3.1. Specific examples

(a) Alkali metal ions: the only reported crystal structure of an alkali metal complexed to an *N*-alkylated amide is that of a Li^+–*N*-methylacetamide complex (Fig. 24) [92]. The crystal structure of the cation $[Li(N\text{-methylacetamide})_4]^+$ has four *N*-methylacetamide ligands in a tetrahedral arrangement around the Li^+ ion. The amide $C_a{=}O$ and $C_a{-}N$ bond lengths are 1.23 and 1.32 Å, respectively, with $C_a{-}C$ bond distance of 1.59 Å. The bond angles in the *N*-methylacetamide ligand are 119, 124 and 117°, for $O{-}C_a{-}N$, $O{-}C_a{-}C$ and $N{-}C_a{-}C$ angles, respectively. The Li–O(amide) bond length is 1.90 Å and the Li–O–C_a angle is 175°.
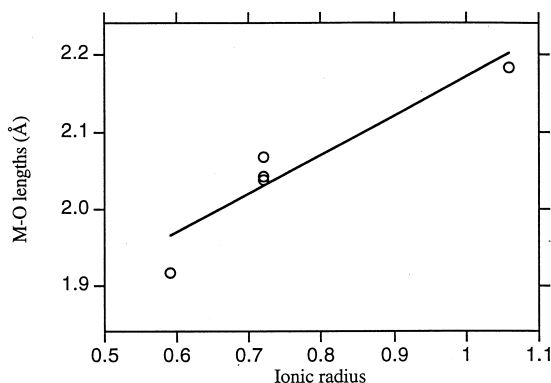
Fig. 23. Plot of M–O versus ionic radius for *O*-bound *N*-alkylamide–metal complexes.

	L
$C_a=O$	1.23 Å
C_a-N	1.32 Å
C_a-C	1.59 Å
O-C_a-N	119 deg
O-C_a-C	124 deg
N-C_a-C	117 deg
Li-O-C_a	175 deg
Li-O-C_a-N	28 deg
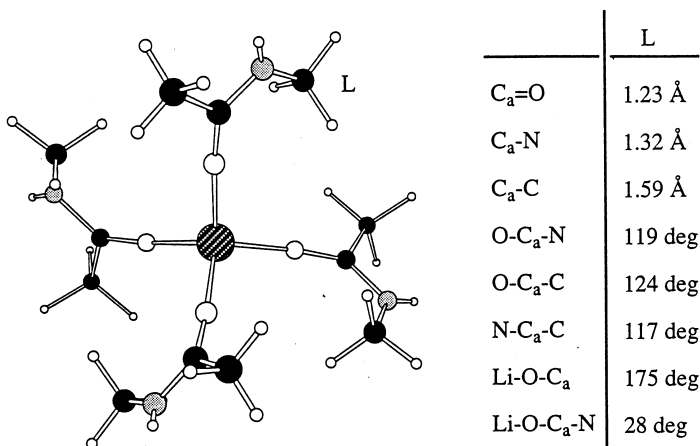
Fig. 24. X-ray crystal structure of the cation $[Li(N\text{-methylacetamide})_4]^+$.

(b) Alkaline earth metal ions: a representative example of an alkaline earth metal complexed to an N-alkylated amide is that of the Mg^{2+} complex, $[Mg(N\text{-methylacetamide})_2(OH_2)_4]^{2+}$. The crystal structure is shown in Fig. 25 [93]. In this complex, the two N-methylacetamide ligands have $C_a=O$ and C_a–N bond lengths of 1.25 and 1.31 Å, respectively, and a C_a–C bond distance of 1.52 Å. The corresponding bond angles in the N-methylacetamide ligand are 120, 123 and 117°, for O–C_a–N, O–C_a–C, and N–C_a–C angles, respectively, and are almost identical to those in the Li^+ complex described above [90]. The two Mg–O bond lengths are similar at 2.05 Å, likewise the two Mg–O–C_a angles are similar at ca. 142°. The Mg–O–C_a–N torsional angle of 18° indicates a weak planar torsional preference in this complex.

	L
$C_a=O$	1.25 Å
C_a-N	1.31 Å
C_a-C	1.51 Å
O-C_a-N	120 deg
O-C_a-C	123 deg
N-C_a-C	117 deg
Mg-O-C_a	142 deg
Mg-O-C_a-N	18 deg

Fig. 25. X-ray crystal structure of the cation $[Mg(N\text{-methylacetamide})_2(OH_2)_4]^{2+}$.

3.4. Metal compounds with N,N-dialkylacetamide

More data are available for metal N,N-dialkylacetamide compounds than are available for either the metal N-alkylacetamide or metal acetamide compounds. Structural features have been analyzed for the 38 instances where N,N-dialkylaceta-mide ligands are bound to metal ions through the amide oxygen. The results of this analysis are presented in Table 5 as a function of four metal ion types observed, alkaline earth (Group 2) compounds, transition metal compounds, 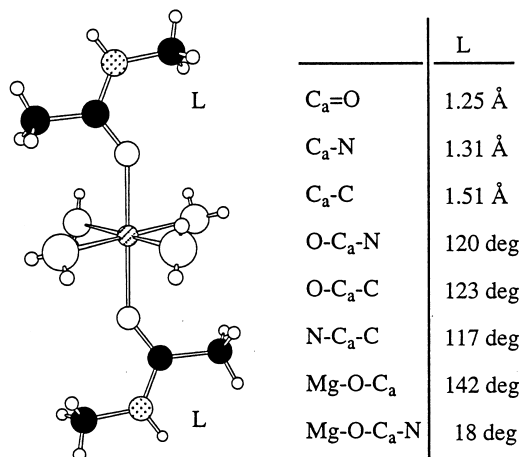trivalent lanthan-ide compounds and tetravalent actinide compounds. Representative structures for each metal ion type are also presented below.

Table 5 reveals several changes in the amide's structure that occur following metal complexation. A marked increase in the average C_a–O bond length as compared with the free N,N-dalkylacetamides is apparent, ranging from 0.02 Å (lanthanide compounds) to 0.06 Å (alkaline earth compounds). Shortening of the average C_a–N bond is observed, ranging from 0.01 Å in the divalent transition metal com-pounds to 0.14 Å for the lanthanide compounds, although the significance of the change in the latter case is obscured by the large scatter in the data.

On average, changes in the O–C_a–N angle vary upon metalation and no consistent trend is apparent. Except for the average O–C_a–N angle in divalent transition metals compounds (decreased by 4°) and O–C_a–C angle (decreased by 3° for tetravalent actinides), a less than one standard deviation in these amide bond angle changes would include the bond angles for the free N,N-dialkylacetamide.

As noted previously for the DMF and acetamide compounds, a striking difference exists in the average M–O–C_a for the divalent transition metal N,N-dialkylacetamide compounds as compared with other metal types. The average divalent transition metal N,N-dialkylacetamide complex possess a fairly acute (132°) M–O–C_a angle as compared with the other average metal N,N-dialkylacetamide compounds, which range from 152 to 159°. Only for the divalent transition metal compounds are most metals found in the amide plane. In all other instances the metal is nonplanar with

Table 5
Structural features of N,N-dialkylacetamide type ligands when attached to a metal ion through oxygen[a]

Metal type	No. of ligands	C_a=O	C_a–N	C_a–C	O–C_a–N	O–C_a–C	N–C_a–C	M–O–C_a	Planar	N-side
None[b]	28	1.23(1)	1.34(2)	1.52(2)	122(1)	120(1)	119(2)	—	—	—
2A	8	1.24(1)	1.30(2)	1.52(3)	122(2)	120(1)	118(1)	151(8)	4/8	0/8
TM^{2+}	7	1.26(1)	1.33(3)	1.51(1)	118(1)	121(2)	120(1)	132(6)	6/7	0/7
Ln^{3+}	11	1.25(3)	1.20(8)	1.59(8)	125(8)	120(3)	115(5)	152(8)	1/11	0/11
An^{4+}	11	1.28(2)	1.32(2)	1.50(2)	119(3)	117(1)	124(3)	158(8)	0/11	0/11

[a]Distances are given in Å and bond angles are given in degrees. Standard deviations (1σ) are given in parentheses. The orientation of the amide is classified as planar if the M–O–C_a–N torsion angle is either $0\pm20°$ or $180\pm20°$. The position of the metal ion is classified as N-side if the M–O–C_a–N torsion angle is $0\pm90°$. Metal ions: 2A (Mg^{2+}, Ca^{2+}), TM^{2+} (Co^{2+},Cu^{2+}, Zn^{2+}, Pt^{2+}), Ln^{3+}, (La^{3+}, Nd^{3+}, Tb^{3+}), An^{4+} (U^{4+}, Th^{4+}).
[b]Values taken from Table 1.
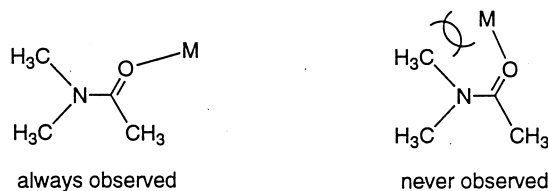
Fig. 26. Metal position in N,N-dialkylacetamide compounds.

respect to the amide either for the majority of that class of metal-compound or exclusively for that class of metal-compound (in the case of the tetravalent actinides). Irregardless of the planarity of the metal amide moiety, with these relatively bulky amides the metal is always found on the opposite site of the carbonyl from the amide nitrogen (Fig. 26).

A plot of the observed M–O(amide) bond length versus. Shannon's ionic radii for the N,N-dialkylacetamide compounds is shown in Fig. 27. A good correlation between the ionic radii and the observed M–O(amide) bond lengths is again observed. A least squares linear regression of the data results in the following equation:

$$y = 1.55 + 0.73x; \quad R = 0.95. \tag{4}$$

3.4.1. Specific examples

(a) Alkaline earth metal ions: the three known crystal structures of alkaline earth metal complexes with N,N-dialkylated amides are those formed with N,N-dimethyla-cetamide [94,95]. These complexes all have octahedral geometries, arranged around either a Mg^{2+} [95] or Ca^{2+} [94] ion. A representative example for this class of metal–amide complexes is shown in Fig. 28 for the octahedral Mg^{2+} complex, $[Mg(N,N\text{-dimethylacetamide})_6]^{2+}$ [95]. In this complex, the amide $C_a{=}O$ and $C_a{-}N$ bond lengths average to 1.24 and 1.30 Å, respectively, and the $C_a{-}C$ bond distance is 1.52 Å. The average bond angles in the amide ligands are 121, 121 and
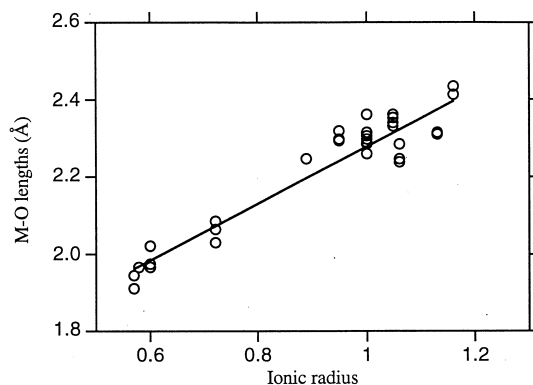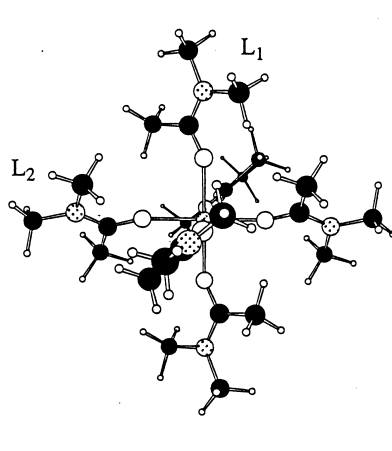
Fig. 27. Plot of M–O versus ionic radius for O-bound N,N-dialkylamide–metal complexes.
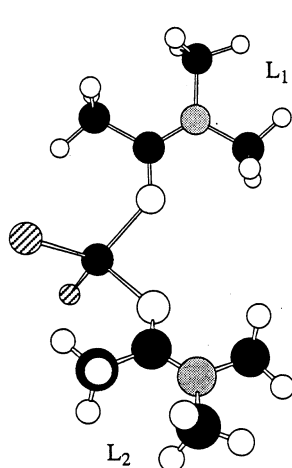
	L_1	L_2
$C_a=O$	1.26 Å	1.23 Å
C_a-N	1.30 Å	1.31 Å
C_a-C	1.53 Å	1.51 Å
O-C_a-N	120 deg	121 deg
O-C_a-C	121 deg	121 deg
N-C_a-C	119 deg	118 deg
Mg-O-C_a	142 deg	158 deg
Mg-O-C_a-N	167 deg	179 deg

Fig. 28. X-ray crystal structure of the cation $[Mg(N,N\text{-dimethylacetamide})_6]^{2+}$.

118°, for the O–C_a–N, O–C_a–C and N–C_a–C angles, respectively. The equatorial Mg–O(amide) bond lengths (2.03 Å) are slightly shorter than those in the axial position (2.08 Å). The Mg–O–C_a bond angles in the N,N-dimethylacetamide complex are 158° (eq) and 142° (ax). The equatorial Mg–O–C_a–N torsional angles of 167° and the axial Mg–O–C_a–N torsional angles of 179°, show a definite planar torsional preference in this example, although this preference occurs only about half of the time in this class of complexes.

(b) Transition metals (+2): a typical example of transitional metal complexes with N,N-dialkylamides is shown in Fig. 29 for the tetrahedral Zn^{2+} complex, $[Zn(N,N\text{-dimethylacetamide})_2Cl_2]$ [96]. In the crystal structure of this complex, the

	L_1	L_2
$C_a=O$	1.26 Å	1.25 Å
C_a-N	1.32 Å	1.32 Å
C_a-C	1.51 Å	1.51 Å
O-C_a-N	119 deg	119 deg
O-C_a-C	121 deg	121 deg
N-C_a-C	120 deg	120 deg
Zn-O-C_a	137 deg	134 deg
Zn-O-C_a-N	176 deg	172 deg

Fig. 29. X-ray crystal structure of $[Zn(N,N\text{-dimethylacetamide})_2Cl_2]$.

amide C_a=O and C_a–N bond lengths are 1.25 and 1.32 Å, respectively, while the C_a–C bond length is 1.51 Å. The average bond angles in the amide ligands are 119, 121 and 120°, for the O–C_a–N, O–C_a–C and N–C_a–C angles, respectively. The shorter Zn–O(amide) bond length of 1.96 Å is associated with the slightly larger Zn–O–C_a angle of 138°, while the longer Zn–O(amide) bond length is associated with the smaller Zn–O–C_a angle of 134°. The average Zn–O–C_a–N torsional angles of 172° highlight the strong planar torsional preference generally found in this class of complexes.

(c) Lanthandes: the crystal structures of three *O*-bound *N,N*-dimethylacetamide complexes with lanthanide metals (Ln) have been reported. The coordination numbers range from 7 to 9. A representative example is shown in Fig. 30 for the 9-coordinate Sm^{3+} complex, [Sm(*N,N*-dimethylacetamide)$_3$(O-NO$_2$)$_3$] [97]. In the crystal structure of this complex, the average amide C_a=O and C_a–N bond lengths are 1.24 and 1.23 Å, respectively, while the average C_a–C bond length is 1.55 Å. The average bond angles in the amide moieties are 126, 120 and 114°, for the O–C_a–N, O–C_a–C and N–C_a–C angles, respectively. These bond angles appear most changed from the average free amide values of 122, 120 and 119°, respectively. The three Sm–O(amide) bond lengths average to ca. 2.32 Å, while the Sm–O–C_a angles range from 140°–155°. Of the three Sm–O–C_a–N torsional angles, two are nonplanar (Sm–O–C_a–N ∼ 117°) while the third is planar (Sm–O–C_a–N torsional angle is 175°). However, as the data in Table 5 shows, *O*-bound Ln–amide complexes in most cases do not have a planar torsional preference.

(d) Actinides (+4): *N,N*-dialkylated amide complexes with tetravalent actinide metal ions are those of U^{4+} and Th^{4+}. There are five reported crystal structures containing one or more mono-coordinated *O*-bound, *N,N*-dialkylamide(s). The coordination number in these complexes range between 6 and 10. A representative example is provided for the tetrakis(isothiocyanato)-thorium(IV) complex, [Th(*N,N*-diisopropylisobutylamide)$_3$(NCS)$_4$] (Fig. 31) [98]. In the crystal structure

	L_1	L_2
C_a=O	1.24 Å	1.21 Å
C_a-N	1.14 Å	1.31 Å
C_a-C	1.62 Å	1.50 Å
O-C_a-N	133 deg	122 deg
O-C_a-C	118 deg	123 deg
N-C_a-C	109 deg	115 deg
Sm-O-C_a	155 deg	152 deg
Sm-O-C_a-N	176 deg	118 deg
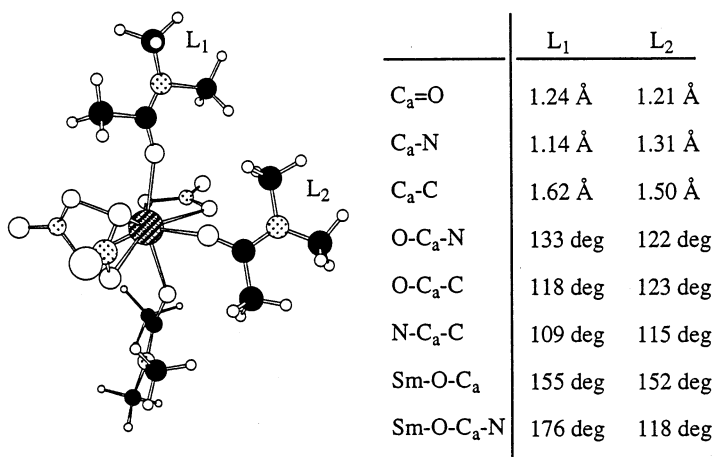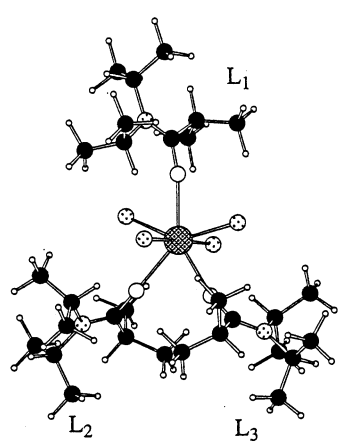
Fig. 30. X-ray crystal structure of [Sm(*N,N*-dimethylacetamide)$_3$(O-NO$_2$)$_3$].

	L_1	L_2	L_3
C_a=O	1.28 Å	1.26 Å	1.26 Å
C_a-N	1.31 Å	1.29 Å	1.31 Å
C_a-C	1.51 Å	1.52 Å	1.49 Å
O-C_a-N	119 deg	120 deg	121 deg
O-C_a-C	115 deg	119 deg	118 deg
N-C_a-C	126 deg	122 deg	121 deg
Th-O-C_a	162 deg	169 deg	162 deg
Th-O-C_a-N	104 deg	136 deg	109 deg

Fig. 31. X-ray crystal structure of [Th(N,N-diisopropylisobutyramide)$_3$(NCS)$_4$].

of this complex, the average amide C_a=O and C_a–N bond lengths are 1.27 and 1.30 Å, respectively, while the average C_a–C bond length is 1.51 Å. The average bond angles in the amide moieties are 120, 117 and 123°, for the O–C_a–N, O–C_a–C and N–C_a–C angles, respectively. The three Th–O–C_a angles are all nearly linear (162, 162 and 169°).

3.5. Metal compounds with N-alkylpyrrolidone

Only nine examples are available for compounds containing N-alkylpyrrolidones bound to metals. The results of the structural analysis are presented in Table 6 for the sole metal ion type observed, divalent transition metals. A representative structure is presented below.

Table 6 reveals that little change in the amide's structure occurs following metal complexation. On average, a slight increase in the average C_a=O bond length (0.02 Å), a slight shortening of the average C_a–N length (0.01 Å), a decrease in the

Table 6
Structural features of N-alkylpyrrollidone type ligands when attached to a metal ion through oxygen[a]

Metal type	No. of ligands	C_a=O	C_a–N	C_a–C	O–C_a–N	O–C_a–C	N–C_a–C	M–O–C_a	Planar	N-side
None[b]	12	1.23(2)	1.33(1)	1.50(2)	125(1)	126(1)	109(1)	—	—	—
TM^{2+}	9	1.25(1)	1.32(1)	1.49(2)	123(3)	127(2)	109(2)	133(5)	7/9	2/9

[a]Distances are given in Å and bond angles are given in degrees. Standard deviations (1σ) are given in parentheses. The orientation of the amide is classified as planar if the M–O–C_a–N torsion angle is either $0 \pm 20°$ or $180 \pm 20°$. The position of the metal ion is classified as N-side if the M–O–C_a–N torsion angle is $0 \pm 90°$. Metal ions: TM^{2+} (Mn^{2+}, Co^{2+}, Cu^{2+}, Cd^{2+}).
[b]Values taken from Table 1.
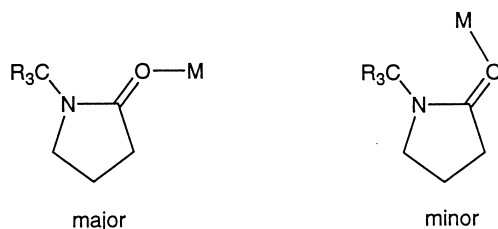
Fig. 32. Metal position in *N*-alkylpyrrolidone compounds.

average O–C_a–N angle (2°), and a slight increase in the average O–C_a–C angle (1°) are observed as compared to the free amides. However, the differences are small; in all instances the average value for the free amides are within one standard deviation of the value for the metal—amide compounds.

The average M–O–C_a angle for the divalent transition metal *N*-alkylpyrrolidone compounds possess the same, fairly acute (133°) value found for the divalent transition metal *N,N*-dialkylacetamide compounds (132°, Table 5). Again, like the metal *N,N*-dialkylacetamide compounds the majority of the metals are found in the amide plane and, in these cases, the metal is always *trans* to nitrogen (Fig. 32).

A plot of the observed M–O(amide) bond length versus. Shannon's ionic radii for the *N*-alkylpyrrolidone compounds is shown in Fig. 33. A good correlation between the ionic radii and the observed M–O(amide) bond lengths is observed with the expected slope of 1 and a high correlation coefficient. A least squares linear regression of the data results in the following equation:

$$y = 1.35 + 1.00x; \quad R = 0.99. \tag{5}$$

3.5.1. Specific example

(a) Transition metals (2+): the crystal structure determinations of *O*-bound *N*-alkylpyrrolidone complexes with Co^{2+} [99,100], Cu^{2+} [101–104], Mn^{2+} [105] and Cd^{2+} [106] have been reported. A representative example is provided in Fig. 34 for
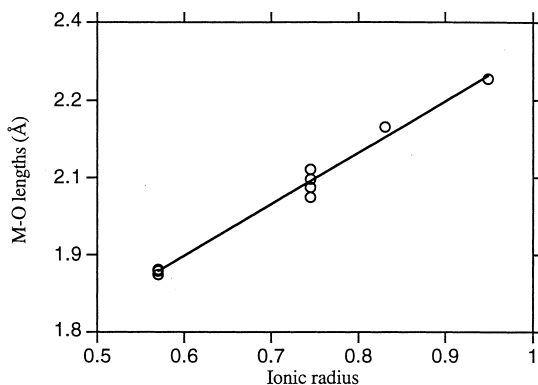
Fig. 33. Plot of M–O versus ionic radius for *O*-bound pyrrolidineamide–metal complexes.

	L
$C_a=O$	1.25 Å
C_a-N	1.33 Å
C_a-C	1.50 Å
O-C_a-N	125 deg
O-C_a-C	126 deg
N-C_a-C	109 deg
Co-O-C_a	131 deg
Co-O-C_a-N	87 deg
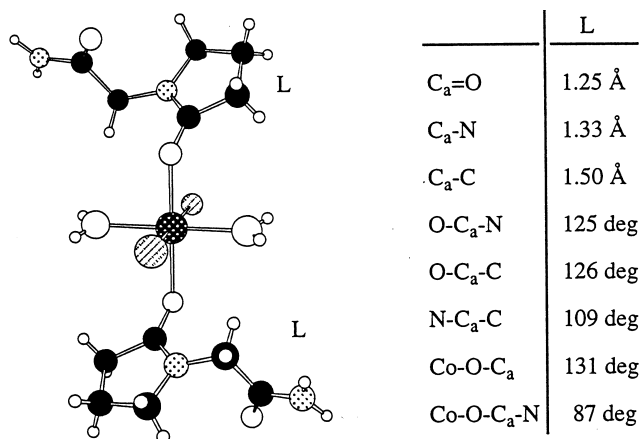
Fig. 34. X-ray crystal structure of [Co(2-oxo-1-pyrrolidineacetamide)$_2$(OH$_2$)$_2$Cl$_2$].

the Co^{2+} complex, [Co(2-oxo-1-pyrrolidinacetamide)$_2$(OH$_2$)$_2$Cl$_2$] [96]. In the crystal structure of this complex, the amide $C_a=O$ and C_a–N bond lengths and 1.25 and 1.33 Å, respectively, while the C_a–C bond length is 1.50 Å. The bond angles in the amide moieties of the 5-membered pyrrole rings are 125, 126 and 109°, for the O–C_a–N, O–C_a–C and N–C_a–C angles, respectively. The two Co–O(amide) bond lengths are similar at 2.12 Å, likewise, the two Co–O–C_a angles are similar at 131°. Unlike the majority of this class of compounds, there is no planar torsional preference apparent in this complex, the Co–O–C_a–N torsional angle is 87°.

4. Nitrogen-bound metal–amide complexes

Metalation of the amide nitrogen requires deprotonation of the amide nitrogen. There are many examples in which multidentate ligands bearing amide functionality are bound to the metal through the amide's nitrogen [2]. Common chelate rings that occur in these ligands are shown in Fig. 35. On the other hand, examples of a metal being nitrogen-bound to a monodentate amide ligand are rare. Only four examples of metal complexes containing nitrogen-bound monodentate amides occur in the CSD. Two were rejected, one because of the unusually poor quality of the
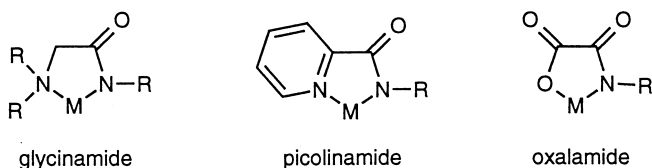
Fig. 35. Common chelate rings that exhibit metal–nitrogen(amide) bonding: glycinamide, picolinamide and oxalamide.

Table 7
Structural features of acetamide when attached to a metal ion through nitrogen[a]

Metal type	No. of ligands	$C_a=O$	$C_a–N$	$C_a–C$	$O–C_a–N$	$O–C_a–C$	$N–C_a–C$	$M–N–C_a$	Planar	trans to CH_3
None[b]	128	1.24(1)	1.33(2)	1.51(2)	122(1)	121(1)	117(1)	—	—	—
Co^{3+}	1	1.27	1.34	1.51	122	119	118	131	1/1	1/1
Pt^{2+}	1	1.27	1.28	1.49	122	116	121	132	1/1	1/1

[a]Distances are given by Å and bond angles are given in degrees. Standard deviations (1σ) are given in parentheses. The orientation of the amide is classified as planar if the $M–N–C_a–O$ torsion angle is either $0\pm20°$ or $180\pm20°$.

crystal structure ($R_{fac}=0.134$) and the second because the amide, being contained in a four membered ring, did not meet the general criteria for inclusion as noted in Section 1.

Table 7 described the bond distances and angles for the two examples examined. In both cases, lengthening of the carbonyl bond by 0.03 Å from the averages $C_a–O$ bond in the free amides was observed. The $C_a–N$ bond distance varied inconsistently in these two instances. In one instance a 0.01 Å increase was observed; in the other a 0.05 Å decrease was found.

The $O–C_a–N$ angle was unchanged in both instances. In both instances the $O–C_a–C$ angle decreased, by either 2° or 5°, and the $N–C_a–C$ angles increased by either 1° or 4°. In both instances a fairly acute (131°–132°) $M–N–C_a$ angle was observed and both examples showed a planar metal–amide arrangement with the metal bound *trans* to the methyl group bound to the carbonyl carbon (Fig. 36).

4.1. Specific example

An example is provided by the square planar Pt^{2+} complex, $[Pt(acetamide)(NH_3)_2 (CH_3CN)]^+$ (Fig. 37) [107]. In the structure of this complex, the $C_a=O$ and $C–N_a$ bond lengths are 1.27 and 1.28 Å, respectively. The $O–C_a–N$ angle is 122°. The $Pt–N_a$ bond length is 2.01 Å, and the $Pt–N–C_a$ angle is 132°. A strong planar torsional preference is found in this complex, with $Pt–N–C_a–O$ of 2°. The structure of the Pt^{2+} complex allows for an intramolecular $C_a=O\cdots H–N$ (2.234 Å) hydrogen-bonding interaction between the hydrogen on the Pt-bound ammonia ligand and the carbonyl oxygen.

Fig. 36. Metal position in *N*-bound amide compounds.

	L
C_a=O	1.27 Å
C_a-N	1.28 Å
C_a-C	1.49 Å
O-C-N_a	122 deg
Pt-N_a-C	132 deg
Pt-N_a-C-O	2 deg
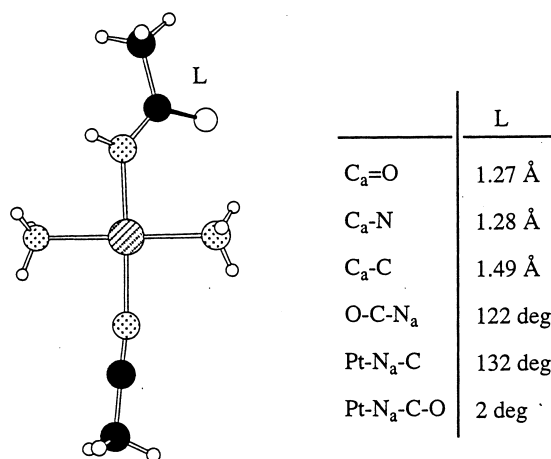
Fig. 37. X-ray crystal structure of the cation [Pt(acetamide-N)(NH$_3$)$_2$(CH$_3$CN)]$^+$.

5. Summary

A survey of monodentate metal–amide complexes in the Cambridge structural database has been performed, and the results presented as a function of the type of binding to the metal (none, oxygen, or nitrogen), the degree of alkylation on the amide, and the type of metal in the metal amide complex. Several aspects involving how the structural features of amide compounds change upon metal coordination have become apparent.

(1) The question of planarity in such simple amides has been the subject of recent attention [108]. For the uncomplexed amides in a condensed phase, it is clear that they possess, within the uncertainty of the data, a planar structure. The structures of these metal amide compounds also indicate that, in general, planarity is retained following metal complexation.

(2) The binding of the amide group to the metal overwhelmingly occurs through the carbonyl oxygen atom rather than the amide nitrogen. Out of the 227 instances examined where monodentate amides were bound to metal ions, in 223 cases the amide was bound to the metal through the carbonyl oxygen atom.

(3) Anticipated changes in average C_a=O and C_a–N bond lengths accompany amide to metal coordination. In general, these changes tend to be on the order of a few hundredths of an angstrom. The observed lengthening of the C_a=O and shortening of the C_a–N bond is consistent with the expected increase in the contribution of the charge-separated resonance form following metal complexation to oxygen.

(4) The relationship between amide and metal contributions to the observed M–O(amide) bond length was examined. The expected correlation of metal ion size to overall M–O bond length was found in plots of M–O(amide) bond length versus the size of the metal ion. For each type of amide, equations were derived that express this relationship. However, the amide contribution to the

M–O(amide) bond length, expressed as the y-intercepts of these equations, spanned a range of 0.24 Å. This variance may be attibuted in part to the uncertainties associated in extrapolation of the data to the y-intercept and in part to the varied steric factors present in the wide variety of complexes examined.

(5) The average values of the M–O–C_a angles depend both on the metal ion type and the degree of alkylation at the carbonyl carbon. With respect to metal type, the metals can be divided roughly into two classes; the divalent transition metals and all other metals. Irrespective of amide type, the divalent transition metals exhibit more acute M–O–C_a angles. In the case of DMF, average M–O–C_a angles are 124° for divalent transition metals and 130 and 145° for other metals. In amides where the carbonyl carbon is alkylated, average M–O–C_a angles range from 133 and 138° for divalent transition metals and 145 and 158° for other metals. As the metal ion typically resides in the plane of the ligand and *trans* to the nitrogen, the increase in M–O–C_a angle with alkylation of the carbonyl carbon can be rationalized by the presence of unfavorable steric interactions between this alkyl group and the rest of the metal complex.

(6) In 158 out of the 223 instances of oxygen-bound amides, the metal is found to be located within 20° of the plane of the amide. Further, with few exceptions (Ln^{3+} and An^{4+} metals with N,N-dialkylacetamides and UO_2^{2+} with acetamide) the majority of any subset of the metal–amide groups examined possess this planar metal–amide structure.

(7) A tendency for the metal to reside *cis* and *trans* with respect to the amide nitrogen is readily rationalized by the steric demands of the ligand. If the amide nitrogen is alkylated (DMF, N-alkylacetamides, N,N-dialkylacetamides and N-alkylpyrrolidones), the steric demands of the amide act to position the metal *trans* to the amide nitrogen atom. Only in the case where the carbonyl carbon is alkylated and the amide is not (acetamide) is this preference reversed.

Acknowledgements

Appendix 1

Reference codes for the structures used in the analysis of the 78 free DMF fragments reported in Table 1

BACRAY10	BARMAI	BONBEL
BOWSOV	BSXDMF	CIWJIB10
CTURCU10	CUFLUK	DECHIC
DIFRAL	DIJNIT	DIJNIT10
FIPREB	FIYBAQ	FODHOV
FOWPOW	GAMFAB	HIJBOR
HTCANF	IPTBNI	JANVEZ
JERDAL	JIGJAK	JIWNIM
JOWVIA	JOWVOG	JUBFER
KADDUO	LADMOS	LELYIK
PIMCOD	PUBFIV	SABNIS
SAKSOM	SAKSOM10	SAVNAE
SEVYAT	SIZJOA	SOHGOL
SYCEDR10	TEHGIW	TEQPUA
VAFTEB	VECTAY	VIZHER
WADDAG	WAKXOV	WASGUS
WAVWAR	WENNOS	WESJUZ
YABPROB	YAPFIE	YATBEA
YONCIN	YUKSOM	YURPEG
YUATCOF	YUVMIL	ZAGPOM
ZAXQAQ	ZEGFEW10	ZEXKAO
ZOJFEJ	ZOZNUX	ZUVYTY

Appendix 2

Reference codes for the structures used in the analysis of the 128 acetamide ligands reported in Table 1

ACEMID01	ACEMID02	ACEMID03
ACEMID05	ADIPAM10	ADROP
AGLUAM10	ALLCAM	ASHCUH
ASPARM	ASPARM02	ASPARM03
ASPARM05	ASPARM06	ASPARM07
ASPCOT	ASPHSC	ASPHSC
AZLMID01	BARBAM	BARKIO10
BEMSER	BHXPAM10	BODCIG
BOHJIR	BOHJIR	CAGNON
CANKEH	CAVFEK	CERNIW
CERYON	CETTOK	CIKSAQ

CIMJEN	CIRYUX	CNRHBR
COSDUJ	COXJII	COSKAB
CPRPCX10	CPRPCX10	CUCRIB
CUVCIF	CYCOAM	DEACAM
DEPRAM	DIHWIA	DIRRIF
DOVGOK	DPPRAM	DUVHOR10
EHMBCX	FECHIE	FEHDAX
FEHDAX01	FESTIG	FIDSEQ
FIDSEQ10	FIRNAV	FOYZIC
GABVOU	GAKSEQ	GEMZED
GIGZUR	GLUTAM01	GLUTAR10
IBURAM	JALHIN01	JATLUL
JAWTIK	KEKGEM	KUGSOU
LAHGAC	LILGES	MNICAM10
NPASPG	OHPHXD	PENHUL
PEVRUD	SIHHOG	SIHHOG10
SUBRAM10	SUCABT	SUCCAM10
TACQUJ	TALVAD	TASGUP
TEHPIF	TEHPOL	TPRACM10
VOHROZ	VUKTEA	WARWIV
WARXES	YAGFUH	YUMLOH
ZAGCUP	ZEJZOD	ZEJZUJ
ZICGUN	ZIGQIO	ZILDON
ZIZDUH	ZOKJAK	ZZZKAY01

Appendix 3

Reference codes for the structures used in the analysis of the 90 *N*-alkylacetamide fragments reported in Table 1

ACENHT	ACEPER	ACGLUA11
ACLACT	ADXPOP	AGALAM01
AGALAM10	ANEUME	AXPTRG
BABSUS	BABTAZ	BAVVUP
BAVWAW	BAVWEA	BAYFOW
BEBVAF	BECGOF	BIKWOH10
CEGKII	CEHKIJ	COWNOR
COXJII	COXJII	DAMEDA
DECTAG	DESBAE	FACPUU
FESKOD	FUDMIA	FUGHEU
GATXOO	GIDFAA	GIDZEY
GIMJER	HANNOZ	HANNUF
HAVDIR	HAZTUX	KEGBED
KEGBIH	KINCOZ	KOYWOK

MADXHP	MELATN	MELATN01
MELATN02	NACMAN10	NPGAMM
PIJGUK	SESVOG	SESVUH
SESVUH	SIALAC	SILDIA
TAGHOY	VATFEB	VEFZIP
VERLUZ	VEVGIM	VOCLAA
VOHNEL	WABSUN	WAFMOF
WEHSOR	WERNOW	WEWNAN
WIBFOC	YELGIF	VOHLEM
YOLKUF	YOMVIF	YOXGEX
YUKVAB	YUKVEF	ZAYKIT
ZEBXEJ	ZEQZUO	ZORAOV

Appendix 4

Reference codes for the structures used in the analysis of the 28 *N,N*-dialkylacetamide fragments reported in Table 1

IHDUR	BIXKIC	CUBYUT
CUHNUO10	CUSRAJ	DABORR
DOJHEP	FALKAE	GEBNIK
JUTSIA	JUTSIA10	KANTIC
KOSZAT	KOTZOI	KOVZOK
KOYNER	KUMYEW	MTCDCX
NADLIN	SIKROT	SIKRUZ
SIKSAG	SOCJAV	VEMFUO
WEWJIR	ZOVGAS	-

Appendix 5

Reference codes for the structures used in the analysis of the 12 *N*-alkylpyrrolidonhe fragments reported in Table 1

COBMOV	COFBUU10	FENPUJ
FESBAS10	GAMBOL	JIKJOC
KOYPET	MPOCUC10	ZACHUG

Appendix 6

Reference codes for the divalent transition metal–DMF compounds

AEOXCU	Cu
ANTHCU	Cu

BALPEJ	Cu
BAWXIG	Fe
CAPPEO	Cu
CIPCOT	Fe
CMFLPT	Pt
CMSFEF10	Cu
COXPEK	Co
CPMOZO	Zn
DOESCF10	Co
DUPFID	Cu
DUPFID10	Co
DUPFID	Cu
DUPFID10	Cu
FACVEK	Ni
FEXWIO	Zn
FOLYAG	Cu
FOZSAO	Zn
FUTKUA	Co
GAZGET	Fe
GEPBAE	Mn
GEPBEI	Co
GETJAQ	Rh
GEXPOO	Cu
GEXPUU	Cu
GEXRAC	Cu
GEYGIA	Mo
GEZWEN	Cu
HEJVUN	Zn
JAFFAX	Co
JAVBAJ	Cu
KETMIF	Cu
KIDNOA	Cd
KOBWIH	Zn
PEDMAM	Cu
PIPKOO	Cu
SAVMUX	Mo
SAVNAE	Mo
SEVYAT	Fe
SEVYEX	Co
VAWSUH	Fe
VIKMOR	Cd
VIKMUX	Cd
VOYRIK	Pt
WEHGEV	Fe
WILCID	Zn

YUTNIK	Ru
ZEWGIR	Ni
ZEWGOX	Cd
ZEZLOF	Ni
ZIPFEJ	Cu
ZUDQEU	Co
ZUZPEP	Ni

Appendix 7

Reference codes for metal–DMF compounds (excluding divalent transition metals)

Group 1 DMF structures

PEKWAD	Na
ZUFFUB	Na
ZUZROB	Li

Group 2 DMF structures

COBHIK	Ca
JUWJUG	Ca
MFPDMG	Mg
TAQSEJ	Ca
ZIMMOX	Mg

Transition metals (+3) DMF structures

BEZFAN10	Re
CADMO	Rh
DERZIJ	Mn
DMFAFE	Fe
FPOLCR	Cr
GIDSOB	Re
JEGJEF	V
PIMTOU	V
TATYIW	V

Transition metals (+4) DMF structures

DIJNIT	V
DIJNIT10	V
FEXFIX	Ti
FEXFOD	Ti

JEBJIJ	V
TABCAA	Zr
VEHLOJ	Zr
VINHEF	Zr

Lanthanide (+3) DMF structures

HELHOV	La
HALBIL	La
SOTXEE	Nd
WIGNAB	La
ZUFOUM	Tb

Actinide (iv) DMF structures

BIXXUB10	Th
BOMJUI	U
COHSAT	Th
GASTID	U
TROPTH	Th

Uranyl ion dmf structures

BOHMUG	UO_2^{2+}
DAZPAV	UO_2^{2+}
DEDCEU	UO_2^{2+}
JEJTEX	UO_2^{2+}
LATVOR	UO_2^{2+}
SEZDUW	UO_2^{2+}
VAXKAG	UO_2^{2+}

Appendix 8

Reference codes for metal acetamide complexes

Transition metals (+2)

ACAMNI	Ni
BAXFIP	Re
FELHOT	Mo
JERDEP	Co

Urnayl complexes

FEPFAHKESJOH

Appendix 9

Reference codes for metal *N*-alkylacetamide complexes

Group 1 metals

LICMAC	Li

Group 2 metals

DURSAK	Mg
DURSEO	Ca
NMALIE	Mg

Appendix 10

Reference codes for metal *N,N*-dialkylacetamide complexes

Group 2

YEMNOT	Mg
ZOWKAX	Ca
ZOWKIF	Ca

Divalent transition metals

CMACCO	Co
DMACCU	Cu
DMAMZN	Zn
DUSHOO	Pt

Lanthanides

CAXYIJ	La
CIDJUU	Sm
CIDKAB	Er

Actinides (+4)

BECVAG	U
CAHCET	U
COJPAS	U
WADMIX	Th
WADMOD	Th

Appendix 11

Reference codes for metal *N*-alkylpyrrolidones complexes

Divalent transition metals

HAFSAI	Co
LEDZUP	Mn
MPOCUC	Cu
SAJKOD	Co
ZACHUG	Cd

Appendix 12

Reference codes for N-bound metal amide complexes

AMCOAC	Co^{3+}
YIRKUF	Pt^{2+}

NOTE: There are ONLY two other structures that could have been included, but were not:

HGACAM Hg^{2+} bis acetamide — rejected due to $R_{fac} = 0.134$
JEJGOU Hg^{2+} — rejected because amide is propriolactam, a four-membered ring case

References

[1] J. Zabicky, The Chemistry of Amides, Interscience, New York, 1970.
[2] H. Sigel, R.B. Martin, Chem. Rev. 82 (1982) 385.
[3] Y.-S. Wang, C.-H. Shen, Y.-H. Yang, J.-K. Zhu, B.-R. Bao, J. Radioanal, Nucl. Chem. Lett. 213 (1996) 199.
[4] Y.-S. Wang, G.-X. Sun, D.-F. Xie, B.-R. Bao, W.-G. Cao, J. Radioanal. Nucl. Chem. Lett. 214 (1996) 67.
[5] G. Thiollet, C. Musikas, Solv. Extra. Ion Exch. 7 (1989) 813.
[6] Q. Tian, M.A. Hughes, Hydrometallurgy 36 (1994) 79.

[7] C. Shen, B. Bao, J. Zhu, Y. Wang, Z. Cao, J. Radioanal, Nucl. Chem. Lett. 212 (1996) 187.

[8] Y. Sasaki, G. Choppin, J. Radioanal, Nucl. Chem. 207 (1996) 383.

[9] P.B. Ruikar, M.S. Nagar, M.S. Subramanian, K.K. Gupta, N. Varadarajan, R.K. Singh, J. Radioanal. Nucl. Chem. Lett. 201 (1995) 125.

[10] P.B. Ruikar, M.S. Nagar, S.A. Pai, M.S. Subramanian, J. Radioanal. Nucl. Chem. 150 (1991) 473.

[11] D.R. Prabhu, G.R. Mahajan, G.M. Nair, M.S. Subramanian, Radiochim. Acta 60 (1993) 109.

[12] L. Nigond, N. Coudamines, P.Y. Cordier, J. Livet, C. Madic, C. Cuillerdier, C. Musikas, Sep. Sci. Technol. 30 (1995) 2075.

[13] L. Nigond, C. Musikas, C. Cuillerdier, Solv. Extr. Ion Exch. 12 (1994) 297.

[14] G.M. Nair, D.R. Prabhu, G.H. Mahajan, J.P. Shukla, Solv. Extr. Ion Exch. 11 (1993) 831.

[15] G.M. Nair, G.R. Mahajan, D.R. Prabhu, J. Radioanal, Nucl. Chem. 1991 (1995) 323.

[16] T. Nakamura, C. Miyake, Solv. Extr. Ion Exch. 13 (1995) 253.

[17] C. Pohlandt, J.S. Fritz, Talanta 26 (1979) 395.

[18] C. Musikas, Sep. Sci. Technol. 23 (1988) 1211.

[19] C. Musikas, Inorg. Chim. Acta 140 (1987) 197.

[20] C. Musikas, H. Hubert, Solv. Extr. Ion Exch. 5 (1987) 977.

[21] B.N. Laskorin, V.V. Yashin, E.A. Filippov, G.M. Chumakova, V.A. Belov, G.G. Arkhipova, Sov. Radiochem. 20 (1978) 438.

[22] G.M. Gasparini, G. Grossi, Process for separation of metals using dialkyl substituted amides, Patent GB2183078A, 1987.

[23] G.M. Gasparini, G. Grossi, Solv. Extr. Ion Exch. 4 (1986) 1233.

[24] G.M. Gasparini, G. Grossi, Sep. Sci. Technol. 15 (1980) 825.

[25] J.S. Fritz, G.M. Orf, Anal. Chem. 47 (1975) 2043.

[26] C. Cuillerdier, C. Musikas, L. Nigond, Sep. Sci. Technol. 28 (1993) 155.

[27] C. Cuillerdier, C. Musikas, P. Hoel, L. Higond, X. Vitart, Sep. Sci. Technol. 26 (1991) 1229.

[28] N. Condamines, C. Musikas, Solv. Extr. Ion Exch. 10 (1992) 69.

[29] M.C. Charbonnel, C. Musikas, Solv. Extr. Ion Exch. 7 (1989) 1007.

[30] G.Y.S. Chan, M.G.B. Drew, M.J. Hudson, P.B. Iveson, J.-O. Lijenzin, M. Skalberg, L. Spjuth, C. Madic, J. Chem. Soc., Dalton Trans. (1997) 649.

[31] B. Boron, S. Chaohong, B. Yizhi, W. Gaodong, Q. Jun, C. Zhengbai, J. Radioanal. Nucl. Chem. 178 (1994) 99.

[32] P. Beer, M.G.B. Drew, A. Grieve, M. Kan, P.B. Leeson, G. Nicholson, M.I. Ogden, G. Willilams, J. Chem. Soc., Chem. Commun. (1996) 1117.

[33] S. Aime, P.L. Anelli, M. Botta, F. Fedeli, M. Grandi, P. Paoli, F. Uggeri, Inorg. Chem. 31 (1992) 2422.

[34] C. Geze, C. Mouro, F. Hindre, M. Le Plouzennec, C. Moinet, R. Rolland, L. Alderighi, A. Vacca, G. Simonneaux, Bull. Soc. Chim. Fr. 133 (1996) 267.

[35] M.S. Konings, W.C. Dow, D.B. Love, K.N. Raymond, S.C. Quay, S.M. Rocklage, Inorg. Chem. 29 (1990) 1488.

[36] J.R. Morrow, S. Amin, C.H. Lake, M.R. Churchill, Inorg. Chem. 32 (1993) 4566.

[37] F.A. Allen, O. Kennard, R. Taylor, Acc. Chem. Res. 16 (1983).

[38] A.E. Martell, R.D. Hancock, Metal Complexes in Aqueous Solution, Plenum Press, New York, 1996.

[39] B.P. Hay, J.R. Rustad, J. Am. Chem. Soc. 116 (1994) 6316.

[40] F.H. Allen, S.A. Bellard, M.D. Brice, B.A. Cartwright, A. Doubleday, H. Higgs, T. Hummelink, B.G. Humelink-Peters, O. Kennard, W.D.S. Motherwell, J.R. Rodgers, D.G. Watson, Acta Crystallogr. B35 (1979) 2331.

[41] N.L. Allinger, K. Chen, M. Raman, A. Pathiaseril, J. Am. Chem. Soc. 113 (1991) 4505.

[42] L.R. Schmitz, N.L. Allinger, J. Am. Chem. Soc. 112 (1990) 8307.

[43] K.B. Wiberg, C.M. Breneman, J. Am. Chem. Soc. 114 (1992) 831.

[44] K.B. Wiberg, K.E. Laidig, J. Am. Chem. Soc. 109 (1987) 5935.

[45] J.-H. Lii, N.L. Allinger, J. Comp. Chem. 12 (1991) 186.

[46] J.-H. Lii, S. Gallion, H. Bender, H. Wilkstrom, N.L. Allinger, K.M. Flurchick, M.M. Teeter, J. Comp. Chem. 10 (1989) 503.

[47] V.P. Manea, K.J. Wilson, J.R. Cable, J. Am. Chem. Soc. 119 (1997) 2033.

[48] L.A. LaPlanche, M.T. Rogers, J. Am. Chem. Soc. 86 (1964) 337.

[49] B.M. Rode, Metal–ligand interactions, in: B. Pullman, N. Goldblum, (Eds.), Organic Chemistry and Biochemistry, Reidel, Dordrecht, 1977.

[50] R.D. Shannon, Acta Crystallogr. Sect. A 32 (1976) 751.

[51] C. Nather, A. John, K. Ruppert, H. Bock, Acta Crystallogr. Sect. C 52 (1996) 1166.

[52] B. Schreiner, K. Dehnicke, D. Fenske, Z. Anorg. Allg. Chem. 619 (1993) 1127.

[53] F. Jiang, M. Hong, X. Xie, R. Cao, B. Kang, D. Wu, H. Liu, Inorg. Chim. Acta 231 (1995) 153.

[54] D. Fenske, G. Baum, H. Wolkers, B. Schreiner, F. Weller, K. Dehnicke, Z. Anorg. Allg. Chem. 619 (1993) 489.

[55] F.J. Hollander, D.H. Templeton, A. Zalkin, Acta Crystallogr. B 29 (1973) 1289.

[56] M. Izumi, K. Ichikawa, M. Suzuki, I. Tanaka, K.W. Rudzinski, Inorg. Chem. 34 (1995) 5388.

[57] C.P. Rao, A.M. Rao, C.N.R. Rao, Inorg. Chem. 23 (1984) 2080.

[58] A.F. Waters, A.H. White, Aust. J. Chem. 49 (1996) 147.

[59] O.S. Roschchupkina, A.V. Bulatov, Y.K. Samovarov, Y.L. Slovokhotov, Y.T. Struchkov, Koord. Khim. 13 (1987) 321.

[60] J.A. Broomhead, J. Evans, W.D. Grumley, M. Sterns, J. Chem. Soc. Dalton Trans. (1977) 173.

[61] C.J. Carrano, M. Mohan, S.M. Holmes, R. de la Rosa, A. Butler, J.M. Charnock, C.D. Garner, Inorg. Chem. 33 (1994) 646.

[62] J. Casebo, J. Marquet, M. Moreno-Manas, M. Prior, F. Teixidor, Polyhedron 6 (1987) 1235.

[63] L. Chichang, L. Shiziong, W. Aihui, J. Huexue, J. Struct. Chem. 2 (1983) 225.

[64] C.L. Hill, M.M. Williamson, Inorg. Chem. 24 (1985) 2836.

[65] E. Kime-Hunt, K. Spartalian, M. DeRusha, C.M. Nunn, C.J. Carrano, Inorg. Chem. 28 (1989) 4392.

[66] E.M. Holt, N.W. Alcock, R.H. Sumner, R.O. Asplund, Cryst. Struct. Comm. 8 (1979) 255.

[67] F.D. Rochon, P.C. Kong, R. Melanson, Can. J. Chem. 61 (1983) 1823.

[68] J.A. Kovacs, R.H. Holm, J. Am. Chem. Soc. 108 (1986) 340.

[69] J.A. Kovacs, R.H. Holm, Inorg. Chem. 26 (1987) 711.

[70] S.I. Troyanov, G.N. Mazo, B.V. Merinov, B.A. Maksimov, Kristallografiya 34 (1989) 235.

[71] U. Castellato, S. Tamburini, P. Tomasin, P.A. Vigato, M. Botta, Inorg. Chim. Acta 247 (1996) 143.

[72] J.-G. Mao, Z.-S. Jin, J.-Z. Ni, J. Huaxue, J. Struct. Chem. 13 (1994) 329.

[73] J. Mao, Z. Jin, Polyhedron 13 (1994) 319.

[74] D.N. Dao, R. Rudert, P. Luger, J. Legendziewicz, G. Oczko, Acta Crystallogr. Sect. G (Cryst. Struct. Commun.) 48 (1992) 449.

[75] J.A. Cunningham, R.E. Sievers, Inorg. Chem. 19 (1980) 595.

[76] J.M. Harrowfield, M.I. Ogden, W.R. Richmond, A.H. White, J. Chem. Soc., Dalton Trans. (1991) 2153.

[77] L. Yang, R. Yang, J. Coord. Chem. 33 (1994) 303.

[78] U. Caesellato, P. Guerriro, S. Tamburini, P.A. Vigato, R. Graziani, J. Chem. Soc., Dalton Trans. (1990) 1533.

[79] N.A. Bailey, D.E. Fenton, C.A. Phillips, U. Casellato, S. Tamburini, P.A. Vigato, R. Graziani, Inorg. Chim. Acta 109 (1985) 91.

[80] P. Charpin, G. Golcher, M. Lance, M. Nierlich, D. Vigner, Acta Crystallogr. Sect. C (Cryst. Struct. Commun.) 41 (1985) 1302.

[81] Z. Da-Chuan, Z. Zhan-Yang, L. Zheng-Jiong, Y. Zhi-Hui, G. Ao-Ling, F. Xi-Zhang, L. Xing-Fu, Acta Crystallogr. Sect. C 49 (1989) 1767.

[82] V.M. Leovac, E.Z. Ivegas, N. Galesic, D. Horvatic, Inorg. Chim. Acta 162 (1989) 277.

[83] D. Mentzafos, A. Hountas, M.A. Tajmir-Riahi, A. Terzis, Acta Crystallogr. Sect. C (Cryst. Struct. Commun.) 43 (1987) 1500.

[84] A. Navaza, M.G. Iroulart, M. Nierlich, M. Lance, J. Vigner, Acta Crystallogr. Sect. C (Cryst. Struct. Commun.) 49 (1993) 1767.

[85] U. Casellato, S. Sitran, S. Tamburini, P.A. Vigato, R. Graziani, Inorg. Chim. Acta 95 (1984) 37.

[86] R.J. Barton, R.W. Dabeka, H. Shengzhi, L.M. Mihichuk, M. Pizzey, B.E. Robertson, W.J. Wallace, Acta Crystallogr. Sect. C 39 (1983) 714.

[87] V.W. Day, J.L. Hoard, J. Am. Chem. Soc. 92 (1970) 3626.

[88] P. Charpin, M. Lance, M. Nierlich, D. Vigner, H. Marquet-Ellis, Acta Crystallogr. Sect. C 44 (1988) 257.

[89] D.J. Kepert, J.M. Patrick, A.H. White, J. Chem. Soc., Dalton Trans. (1983) 381.

[90] V.V. Kravchenko, G.G. Sadikov, N.S. Rukk, E.V. Savinkina, M.G. Zaitseva, L.A. Butman, L.Y. Alikberova, B.D. Stepin, Zh. Neorg. Khim. 34 (1989) 1492.

[91] V.A. Blatov, L.B. Serezhkina, L.G. Makarevich, V.N. Serezhkin, V.K. Trunov, Kristallografiya 34 (1989) 870.

[92] P. Chakrabarti, K. Venkatesan, C.N.R. Rao, Proc. R. Soc. London Ser. A. 127 (1981) 375.

[93] K. Lewinski, L. Lebioda, J. Am. Chem. Soc. 108 (1986) 3693.

[94] K. Lewinski, L. Lebioda, J. Am. Chem. Soc. 108 (1986) 3693.

[95] L. Pavanello, P. Visona, S. Bresadola, G. Bandoli, Z. Kristallogr. 209 (1994) 946.

[96] M. Herceg, J. Fischer, Acta Crystallogr. Sect. B 30 (1974) 1289.

[97] M. de Matheus, J.L. Brianso, X. Solans, G. Germain, J.P. Declercq, Z. Kristallogr. 165 (1983) 233.

[98] K.W. Bagnall, F. Benetollo, E. Forsellini, G. Bombieri, Polyhedron 11 (1992) 1765.

[99] V.S. Sabirov, M.A. Porai-Koshits, Y.T. Struchkov, A.N. Yunuskhodzhaev, Koord. Khim. 18 (1992) 614.

[100] H. Kinoshita, A. Ouchi, Bull. Chem. Soc. Jpn. 61 (1988) 3350.

[101] S.S. Kukalenko, U.T. Struchkov, S.I. Shestakova, A.G. Tsybulevskii, A.S. Batsanov, E.B. Nazarova, Koord. Khim. 9 (1983) 312.

[102] T. Hosokawa, M. Takano, S.-I. Murahashi, H. Ozaki, Y. Kitagawa, K.-I. Sakaguchi, Y. Katsube, J. Chem. Soc., Chem. Commun. (1994) 1433.

[103] L.B. Gan, C.P. Luo, C.H. Huang, G.X. Xu, Q.L. Jin, Chin. Chem. Lett. 3 (1992) 1019.

[104] M.R. Churchill, F.J. Rotella, Inorg. Chem. 18 (1979) 853.

[105] V.K. Sabirov, M.A. Porai-Koshits, Y.T. Struchkov, Koord. Khim. 19 (1993) 38.

[106] G.A. Doyle, D.M.L. Goodgame, S.P.W. Hill, S. Menzer, A. Sinden, D.J. Williams, Inorg. Chem. 34 (1995) 2850.

[107] A. Erzleben, I. Mutikainen, B. Lippert, J. Chem. Soc., Dalton Trans. (1994) 3667.

[108] H.-G. Mack, H. Oberhammer, J. Am. Chem. Soc. 119 (1997) 3567.